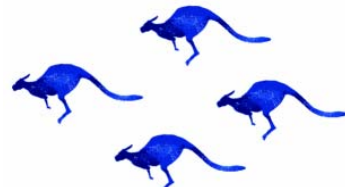


# Ground-based observation of very high energy gamma-rays

Masaki Mori\*

for the CANGAROO team

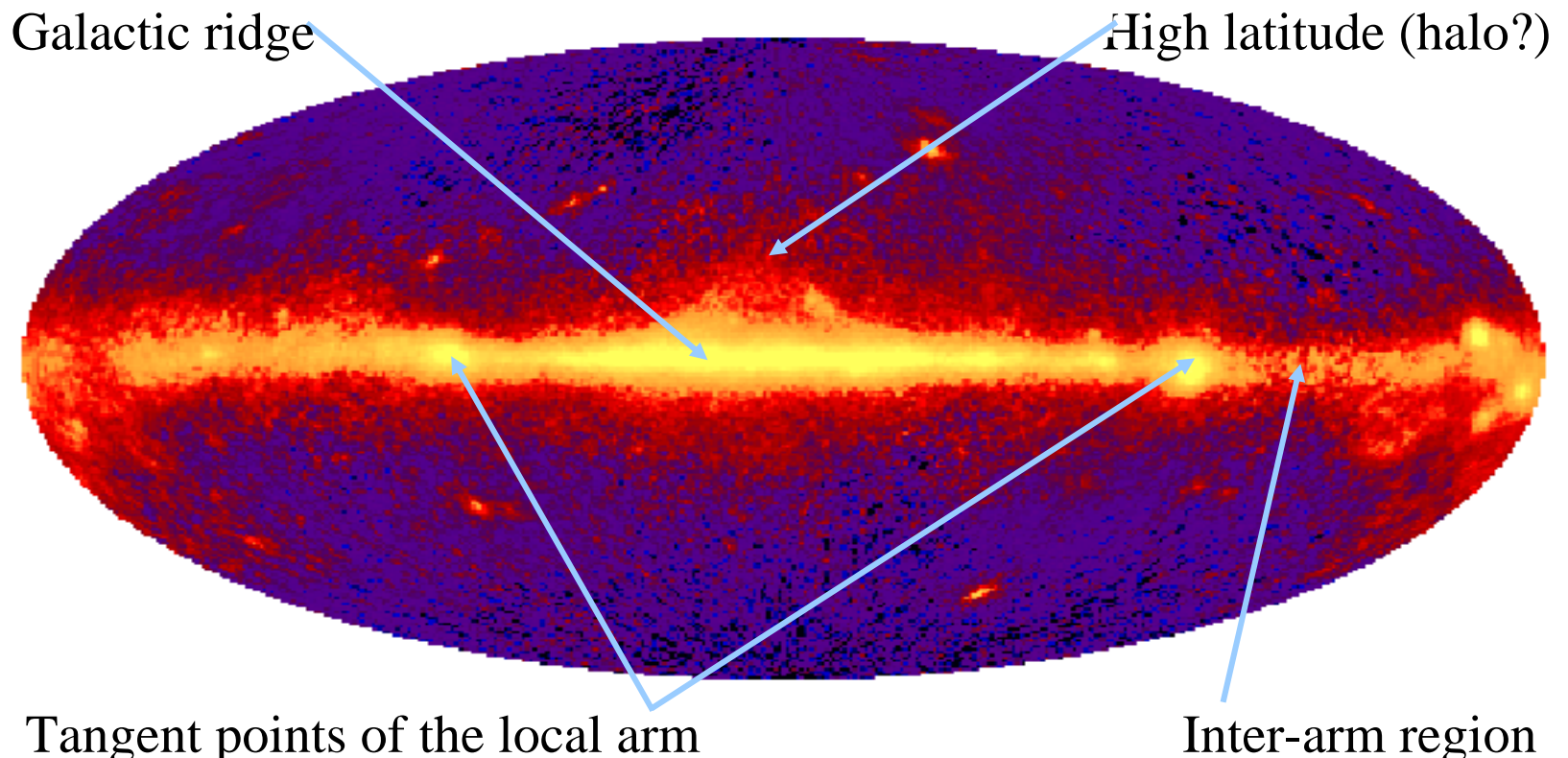
\* *ICRR, The University of Tokyo*



**CANGAROO III**

日本学術振興会 先端研究拠点事業 第1回研究会、2005年12月21-22日、  
名古屋大学野寄記念学術交流館

# GeV gamma-ray sky by EGRET



The dominant feature of the gamma-ray sky is the Galactic diffuse emission, and it is a probe of the *Galactic ISM* and the *CR distributions!*

# The Galactic Diffuse Emission

Straight forward integral over the line-of-sight:

Galactic cosmic-ray distribution of electrons and nucleons (+ He, heavies)

Galactic matter distribution of atomic, molecular, and ionized hydrogen

$$j(E_\gamma, l, b) = \frac{1}{4\pi} \int (c_e \cdot q_{eb} + c_n \cdot q_{nn}) \times (n_{\text{HI}} + n_{H_2} + n_{\text{H II}}) d\rho + \\ \frac{1}{4\pi} \sum_i \int c_e \cdot q_{ic,i} \cdot u_{ic,i} d\rho$$

[ph cm<sup>-2</sup> s<sup>-1</sup> sr<sup>-1</sup> GeV<sup>-1</sup>]

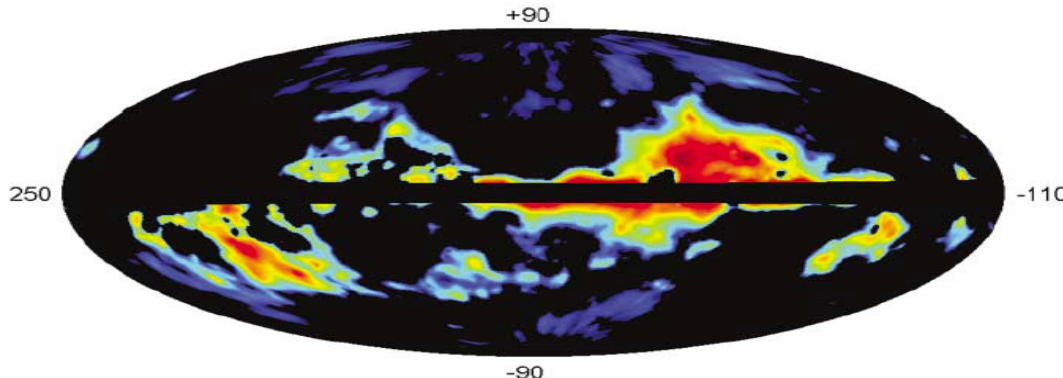
Gamma-ray production functions electron bremsstrahlung, nucleon-nucleon ( $\pi^0$ ), and inverse Compton Synchrotron emission is not significant

Low-energy photon energy density cosmic microwave background, infra-red, visible, and ultraviolet

The hard part: determining the 3-D matter, ISR, and CR distributions.

# Dark gas contribution?

Grenier, Casandjian & Terrier, Science 307, 1292 (2005)

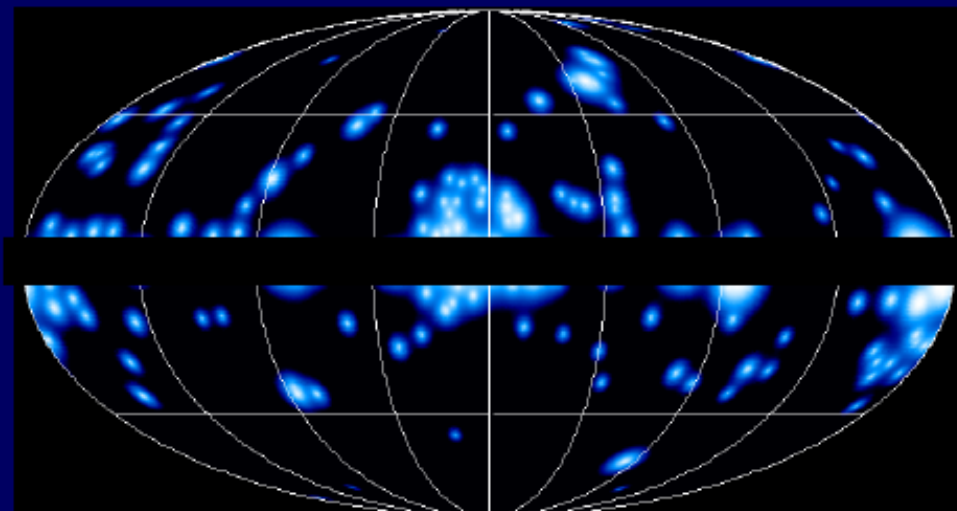


**Clouds of dark gas ( $39\sigma$ )!**  
with  $N(H)$  column-densities  
comparable to  $N(HI)$  and  
 $2N(H_2)$

Grenier & Casandjian, GLAST meeting (Aug. 2005)

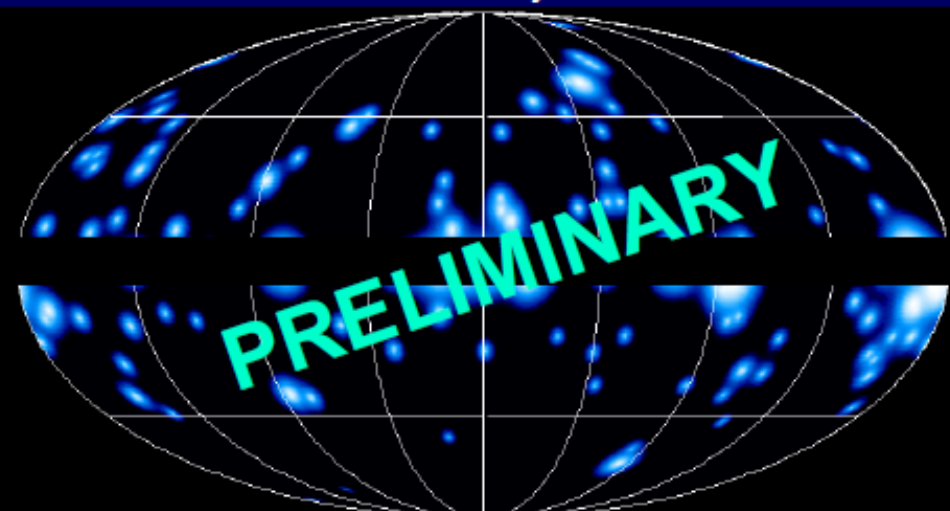
## 3EG persistent EGRET sources

Hartman '99

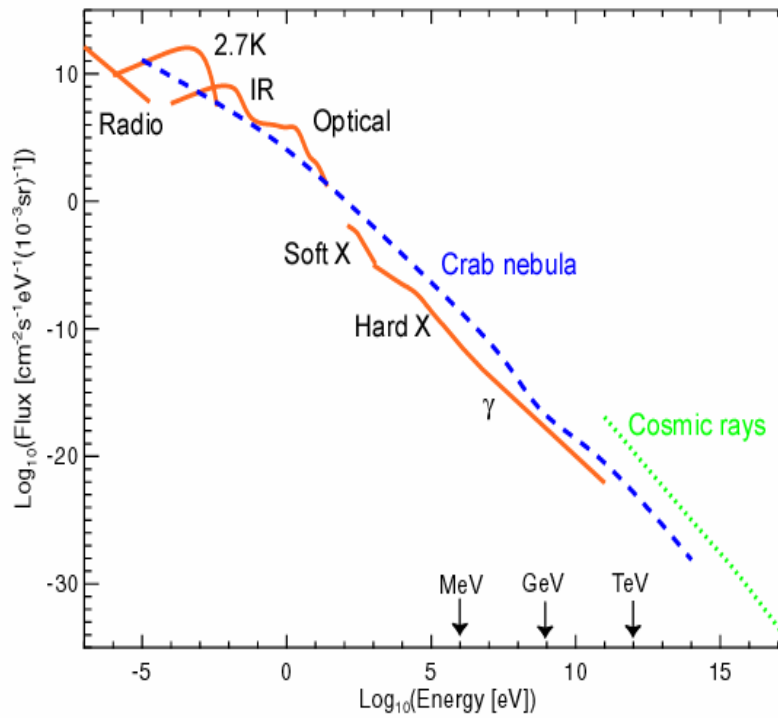


## new persistent EGRET sources

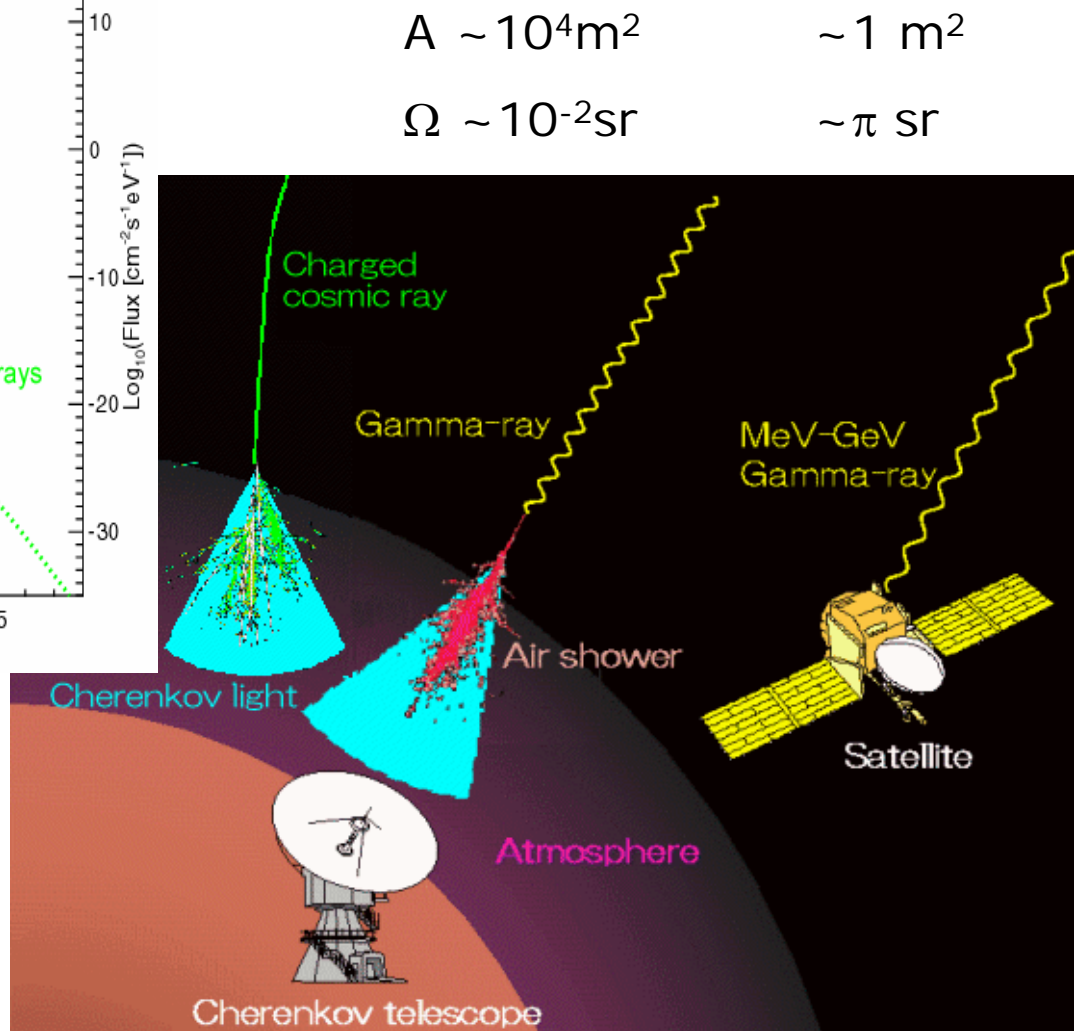
Casandjian '05



# We have to rely on ground-based observation at TeV energies



Diffuse photon spectrum



# Ground-based observation of gamma-rays by atmospheric Cherenkov telescopes

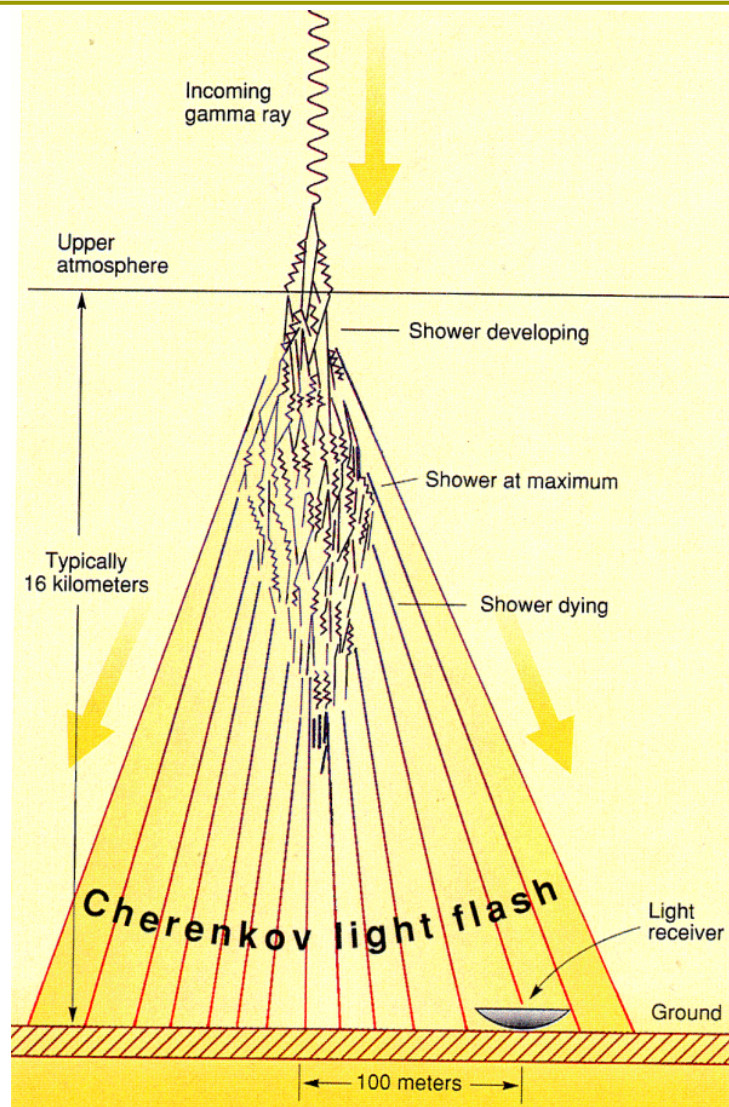
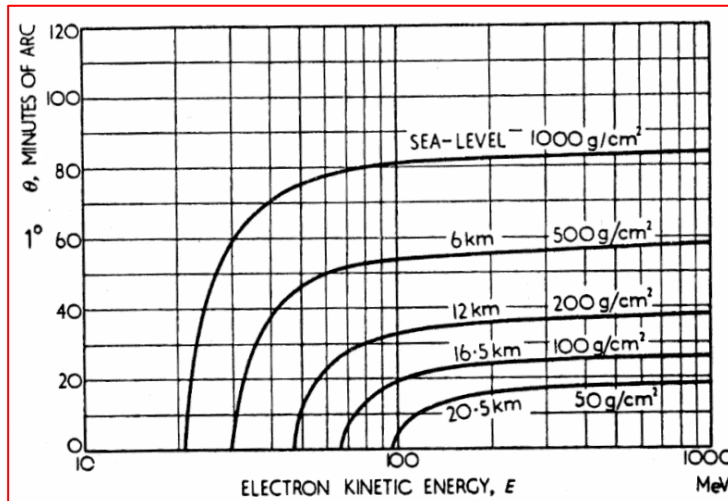
## □ Cherenkov angle

$$\cos \theta = 1/n\beta$$

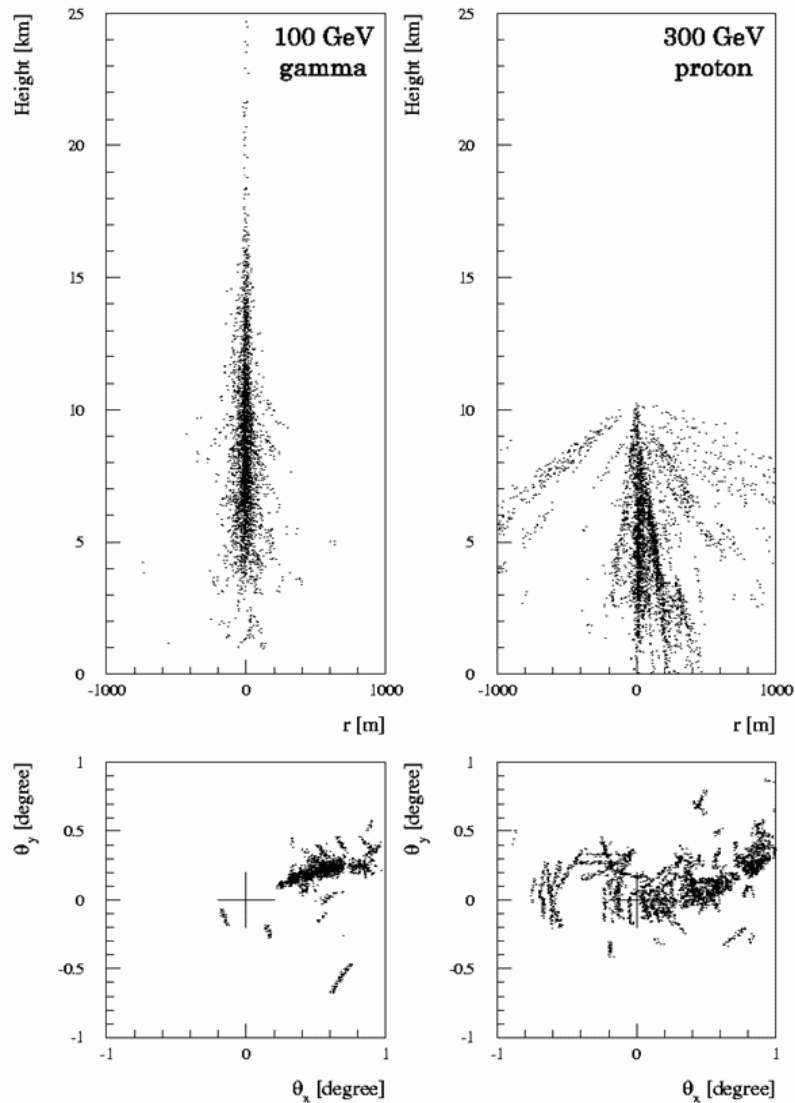
$$\beta = v/c$$

$$n = 1.0003 \text{ (1atm)}$$

$$\Rightarrow \theta = 1.3^\circ \text{ (sea level)}$$



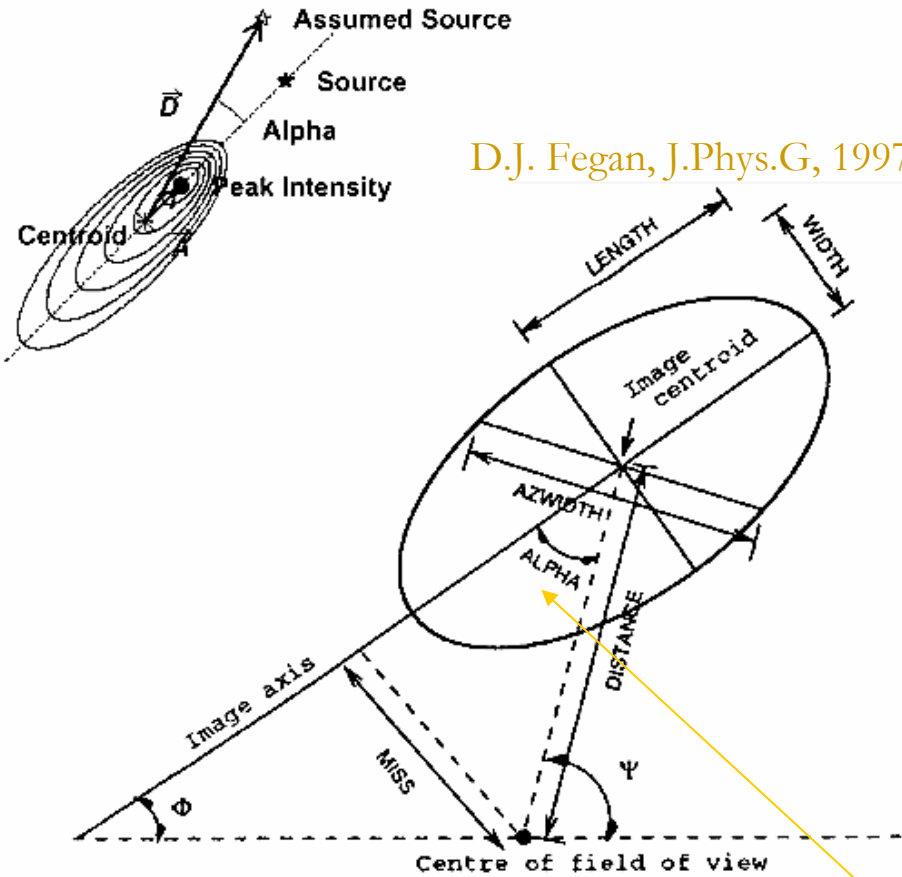
# Rejection of cosmic-ray background by imaging method



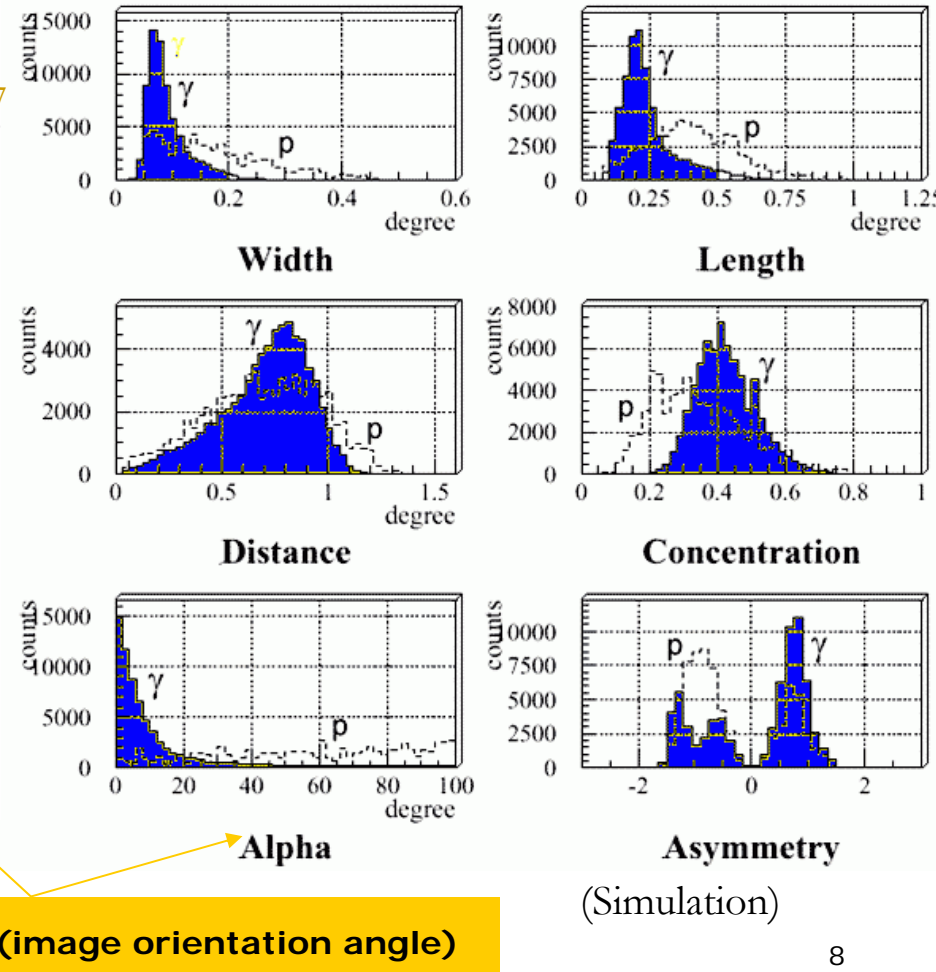
Gamma-rays:  
Electromagnetic  
shower  
 $\Rightarrow$  Sharp image

Protons:  
hadronic shower  
 $\Rightarrow$  Diffuse image

# Imaging analysis



Distribution of imaging parameters



"Image parameters": A.M. Hillas, 1983 ICRC

"Alpha": A.V.Plyasheshnikov and G.F.Bignami, N.C. 1985

# VHE Experimental World

MILAGRO



STACEE



MAGIC



TIBET



MILAGRO

STACEE

VERITAS



MAGIC

TACTIC

TIBET  
ARGO-YBJ

PACT

GRAPES



HESS

CANGAROO III

HESS



CANGAROO



# **“CANGAROO”**

=

**Collaboration of Australia and Nippon for a  
GAmma Ray Observatory in the Outback**



Woomera, South Australia



# CANGAROO team

---

- University of Adelaide 
- Australian National University 
- Ibaraki University 
- Ibaraki Prefectural University 
- Konan University 
- Kyoto University 
- STE Lab, Nagoya University 
- National Astronomical Observatory of Japan 
- Kitasato University 
- Shinshu University 
- Institute of Space and Astronautical Science 
- Tokai University 
- ICRR, University of Tokyo 
- Yamagata University 
- Yamanashi Gakuin University 
- National Inst. Of Radiological Sciences 

# Brief history of CANGAROO

---

- 1987: SN1987A
- 1990: 3.8m telescope
- 1990: ICRR-Adelaide Physics agreement
- 1992: Start obs. of 3.8m tel.
- 1994: PSR 1706-44
- 1998: SNR1006
- 1999: 7m telescope
- 2000: Upgrade to 10m
- 2001: U.Tokyo-U.Adelaide agreement
- 2002: Second and third 10m tel.
- 2004: Four telescope system

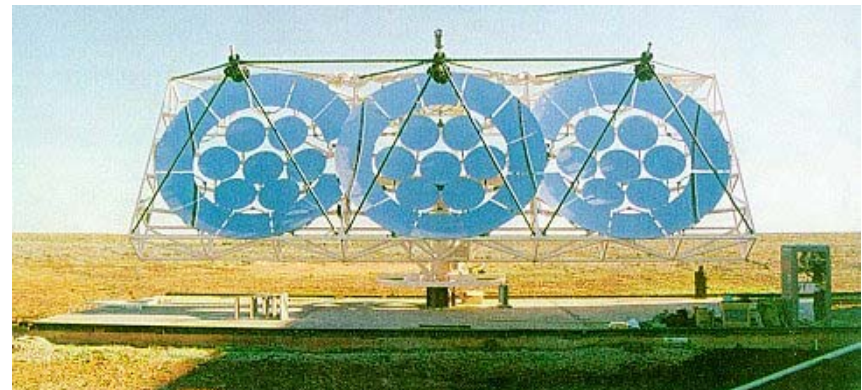
# Why Woomera?

---

- NZ: too wet, not many clear nights
- Woomera:
  - Former rocket range and prohibited area...infra-structure and support
  - Adelaide group was operating BIGRAT



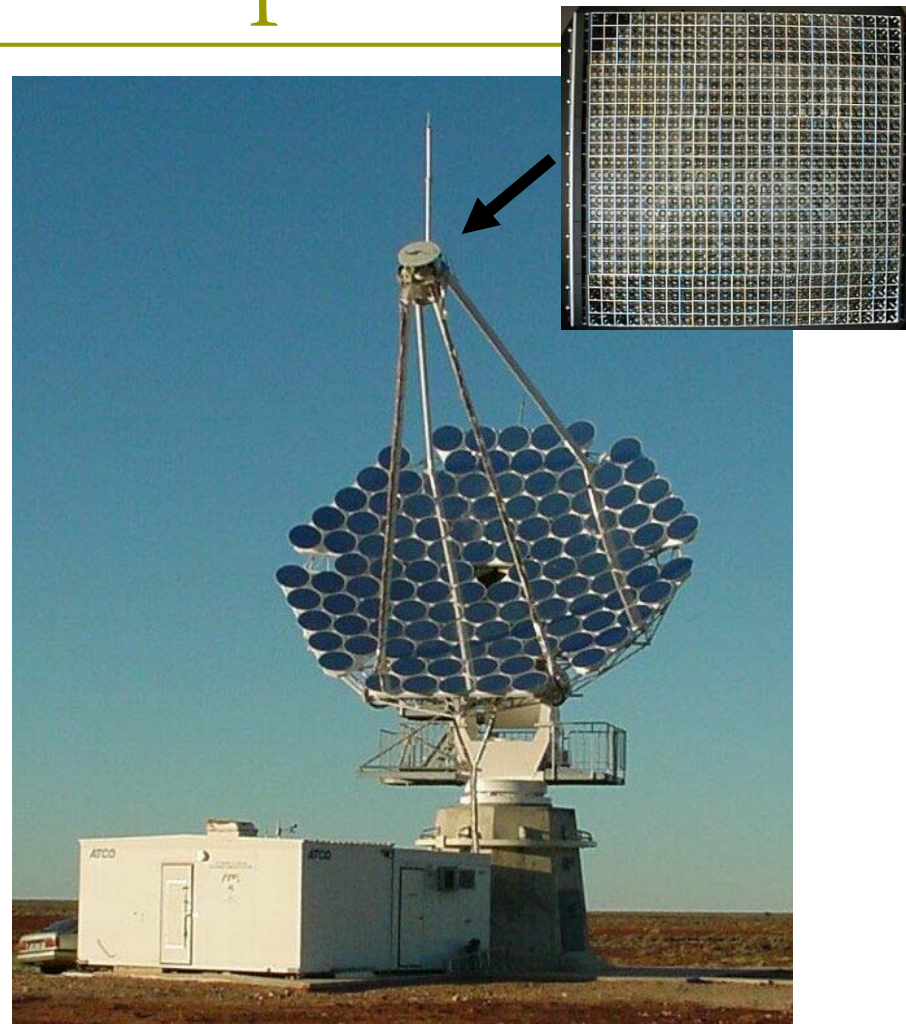
ELDO rocket Launch site in '60s



BIGRAT  
(Bicentennial Gamma Ray Telescope)

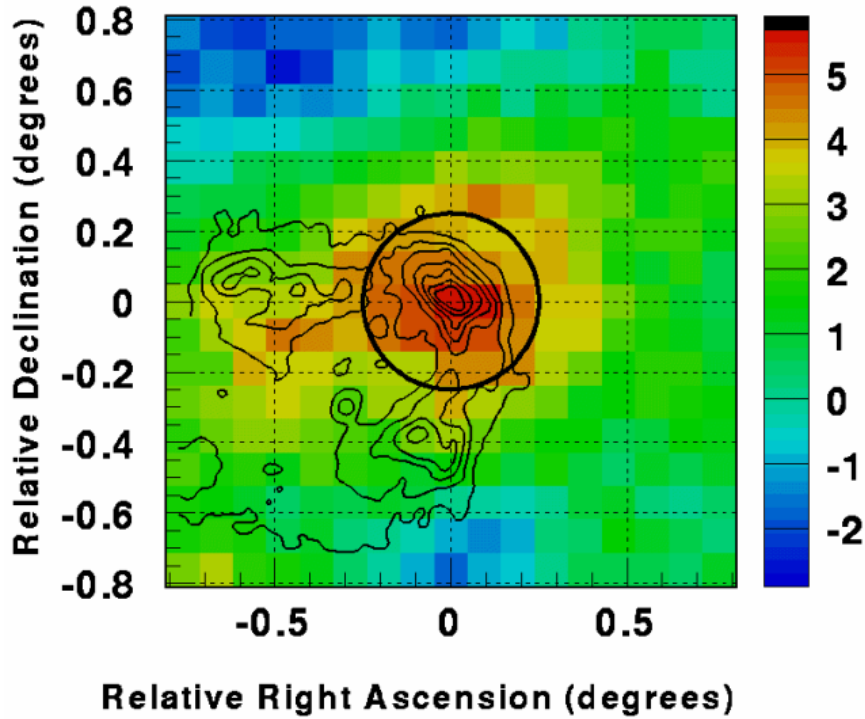
# CANGAROO-II telescope

- Upgraded in 2000 from 7m telescope completed in 1999
- 114 x 80cm CFRP mirror segments  
*(first plastic-base mirror in the world!)*
- Focal length 8m
- Alt-azimuth mount
- 552ch imaging camera
- Charge and timing electronics

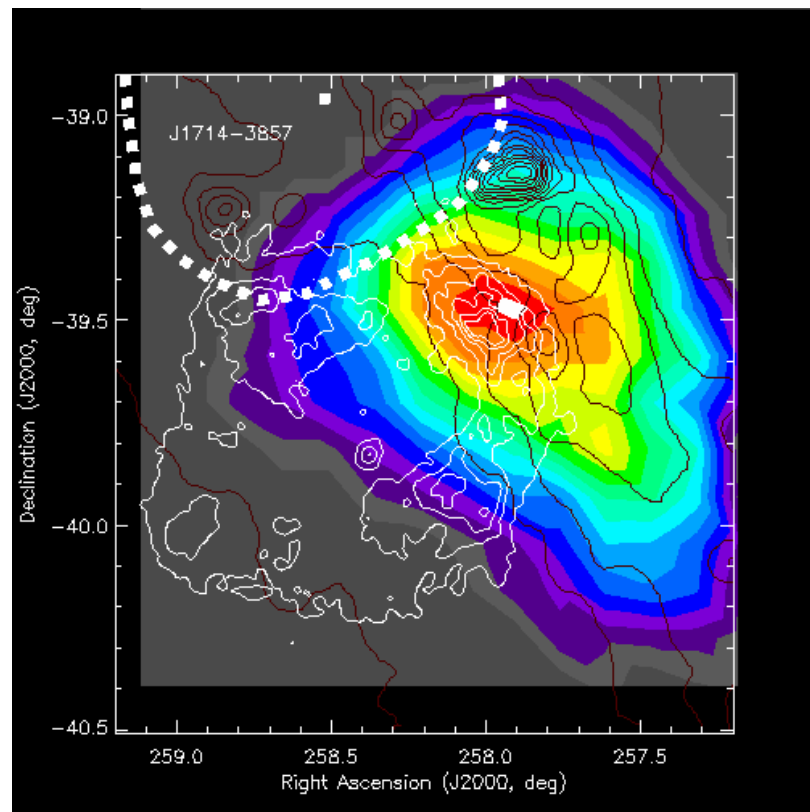


(March 2000)

# SNR RX J1713.7-3946/G347.3-0.5



CANGAROO-I (Muraishi et al., A&A 354, L57, 2000)

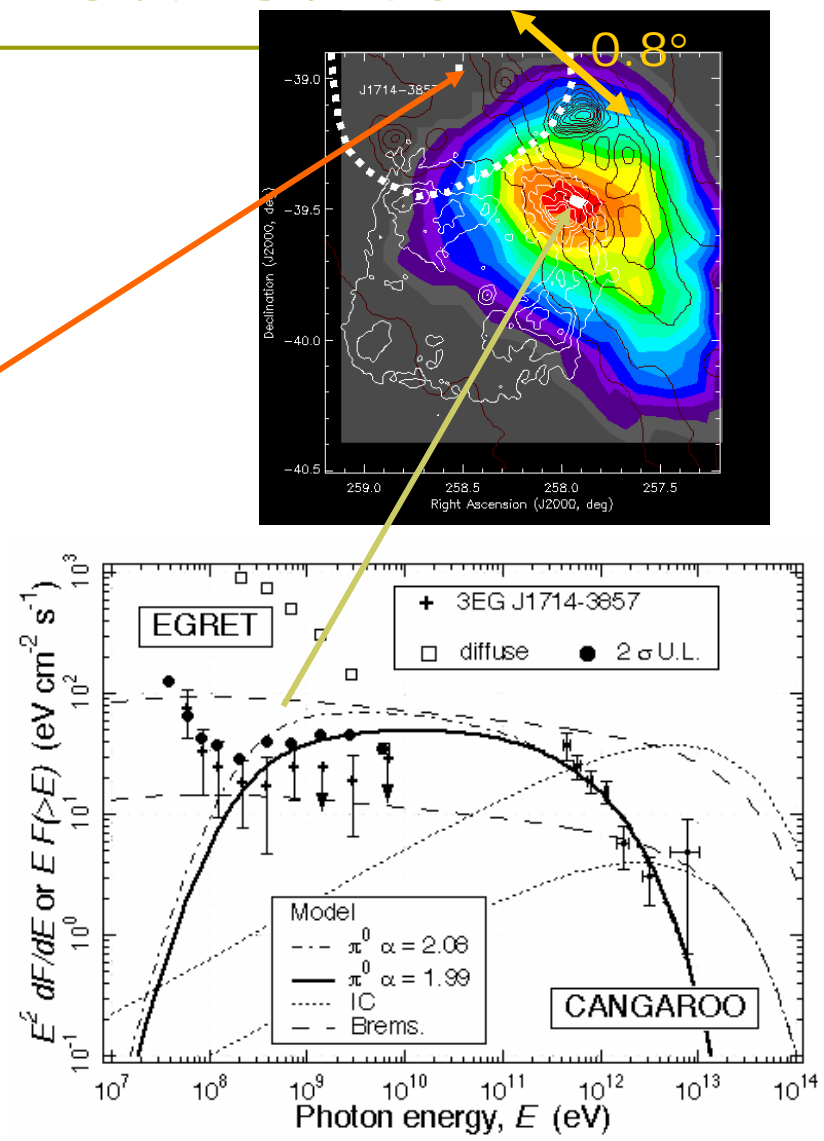
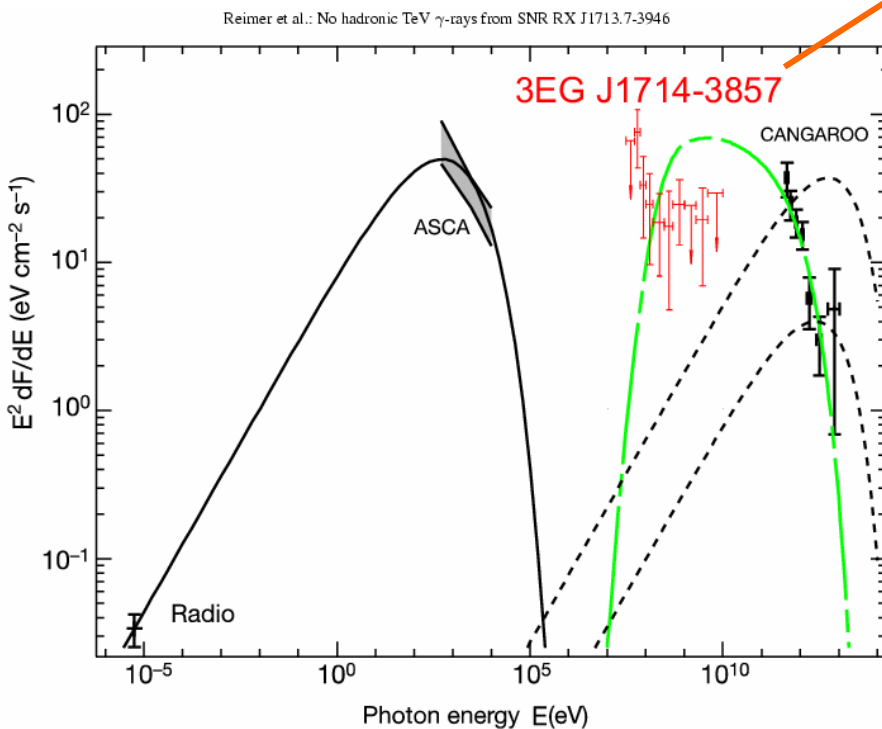


CANGAROO-II (Enomoto et al., Nature 416, 8232002)

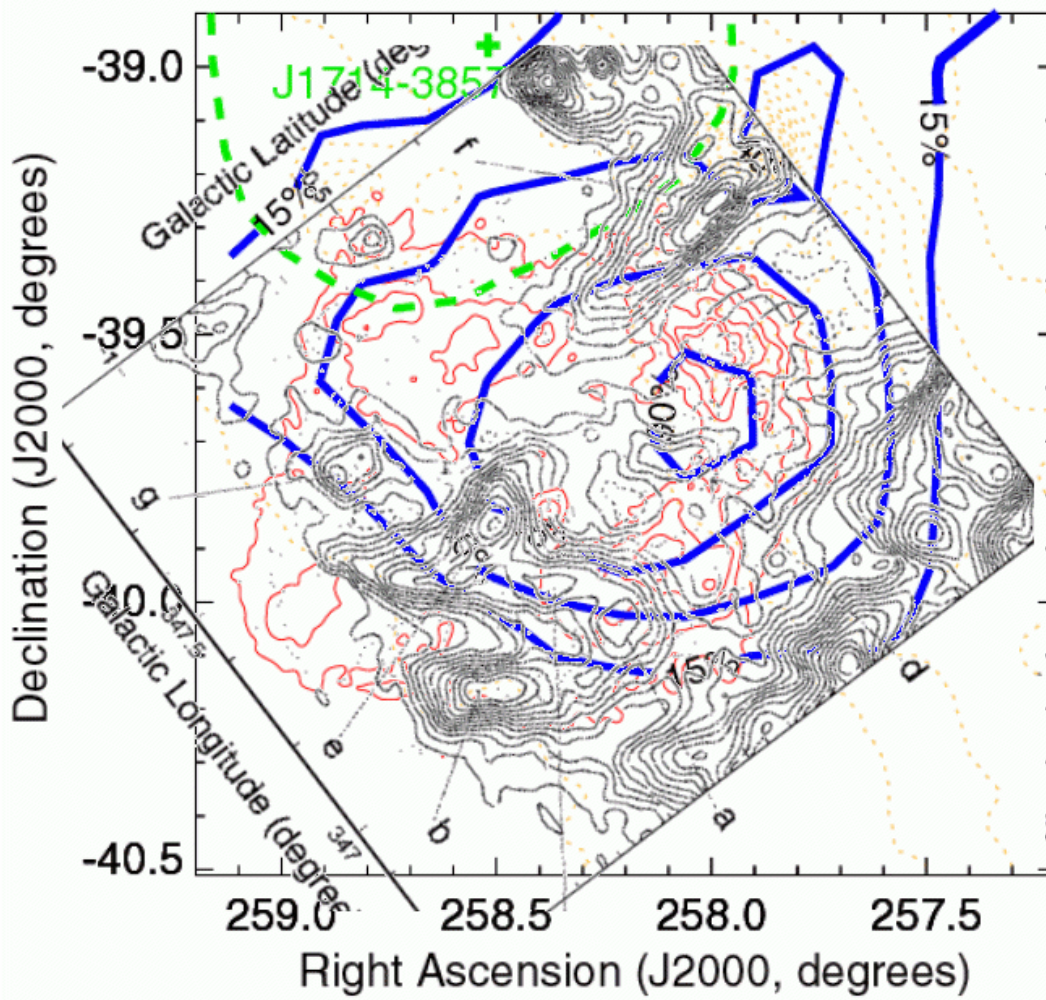
# Spectrum of RX J1713.7-3946

Reimer & Pohl, A&A 390 (2002) L43

Butt et al., Nature 418 (2002) 489



# Correlation with CO -1



RX J1713.7-3946

Blue: TeV  
(CANAGROO)

Green: GeV (EGRET)

Red: X (ROSAT)

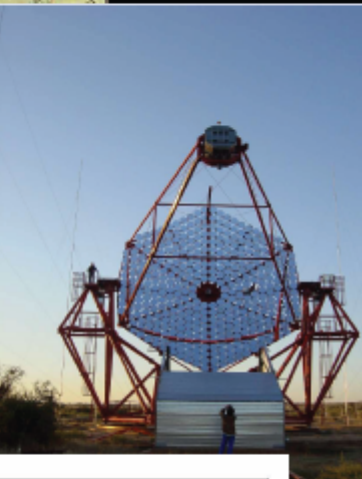
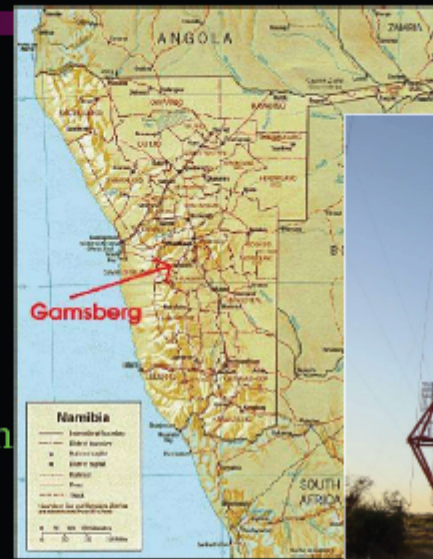
Orange: IR (IRAS)

Black: CO (Nanten)

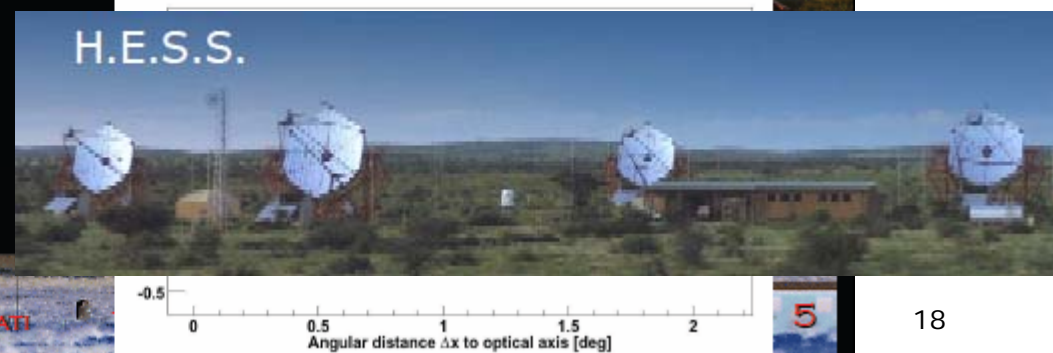
# H.E.S.S.

## HESS PHASE-I ESSENTIAL CHARACTERISTICS

- Four-Telescope network
  - Sited in Namibia,  $23^{\circ}\text{S}$ ,  $15^{\circ}\text{E}$ ,  $1800\text{ m}$  altitude
  - Telescope separation:  $120\text{ m}$
- Telescope Structures
  - Mirror dishes:  $4 \times 107\text{ m}^2$
  - Diameter:  $12\text{ m}$ , Focal length:  $15\text{ m}$
- Mirrors
  - $380 \times 60\text{cm}$  circular facets
  - PSF after alignment ( $r_{80\%}$ )  
 $1.3' / 0.38\text{ mrad}$  on axis
  - Pointing precision  $8''$



H.E.S.S.



# Correlation with CO -2

RX J1713.7-3946

F. Aharonian et al.: The  $\gamma$ -ray supernova remnant RX J1713.7-3946

15

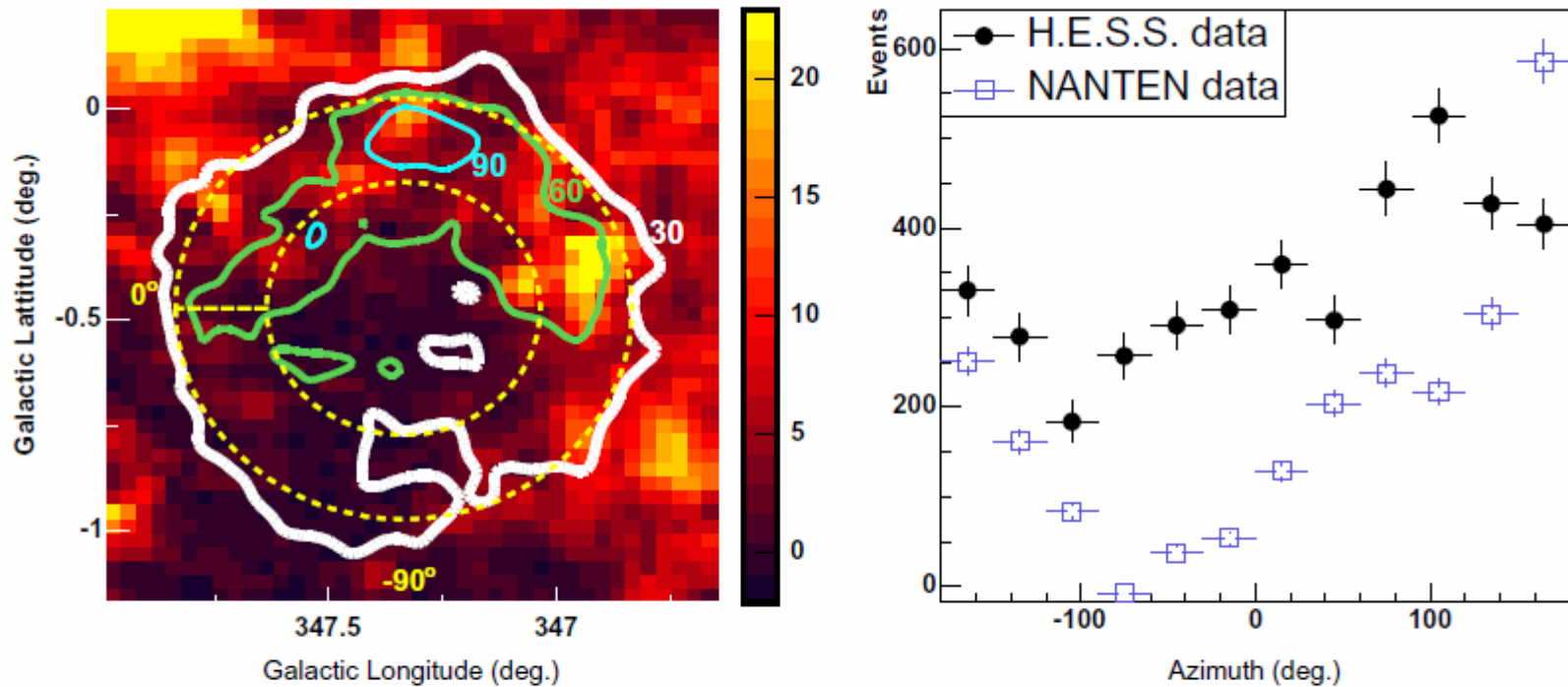


**Fig. 17.** Left panel: Shown are the intensity distribution of CO ( $J = 1 - 0$ ) emission (Fukui et al. 2003) (linear colour scale in units of  $K \text{ km s}^{-1}$ , truncated at a value of 23 to highlight important features), derived by integrating the CO spectra in the velocity range from  $-11 \text{ km s}^{-1}$  to  $-3 \text{ km s}^{-1}$  (which corresponds to 0.4 kpc to 1.5 kpc in space). Overlaid are coloured contours of the H.E.S.S. gamma-ray excess image. The levels are labelled and linearly spaced at 30, 60, and 90 counts. Note that the image is shown in Galactic coordinates. Right panel: Azimuth profile plot, that is, number of counts as a function of the azimuthal angle, integrated in a  $0.2^\circ$ -wide ring covering the shell of RX J1713.7-3946 (dashed yellow circle in the left-hand panel). Plotted are the H.E.S.S. gamma-ray and the NANTEN data set.

# Electrons or protons?

RX J1713.7-3946

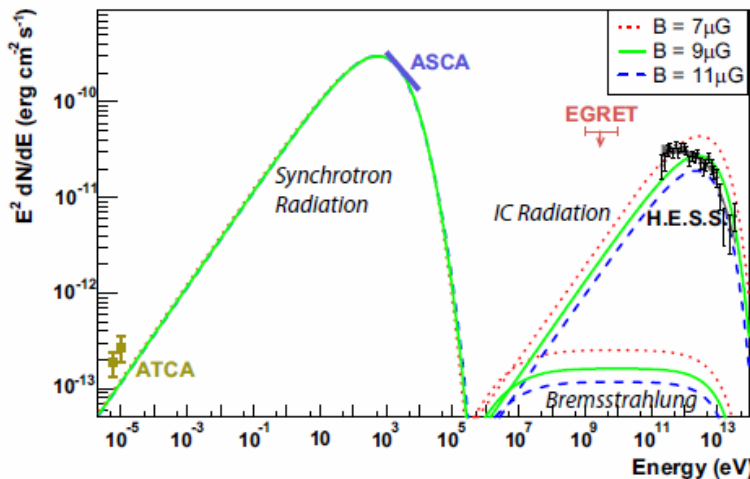


**Fig. 19.** Broadband SED of RX J1713.7–3946. The ATCA radio data and ASCA X-ray data (Hiraga 2005) for the whole SNR are indicated, along with the H.E.S.S. measurement and the EGRET upper limit. Note that the radio flux was determined in Lazendic et al. (2004) for the northwest part of the shell only and was scaled up by a factor of two here to account for the whole SNR. The synchrotron and IC spectra were modelled assuming a source distance of 1 kpc, an age  $T$  of 1000 years, a density  $n$  of  $1 \text{ cm}^{-3}$ , and a production rate of relativistic electrons by the acceleration mechanism in the form of a power law of index  $\alpha = 2$  and an exponential cutoff of  $E_0 = 100 \text{ TeV}$ . Shown are three curves for three values of the mean magnetic field:  $7 \mu\text{G}$ ,  $9 \mu\text{G}$ , and  $11 \mu\text{G}$ , to demonstrate the required range of the  $B$  field strength for this scenario. The electron luminosity is adopted such that the observed X-ray flux level is well matched. For the three magnetic field values the luminosity  $L_e$  is  $L_e = 1.77 \times 10^{37} \text{ erg s}^{-1}$  ( $7 \mu\text{G}$ ),  $L_e = 1.14 \times 10^{37} \text{ erg s}^{-1}$  ( $9 \mu\text{G}$ ), and  $L_e = 0.81 \times 10^{37} \text{ erg s}^{-1}$  ( $11 \mu\text{G}$ ).

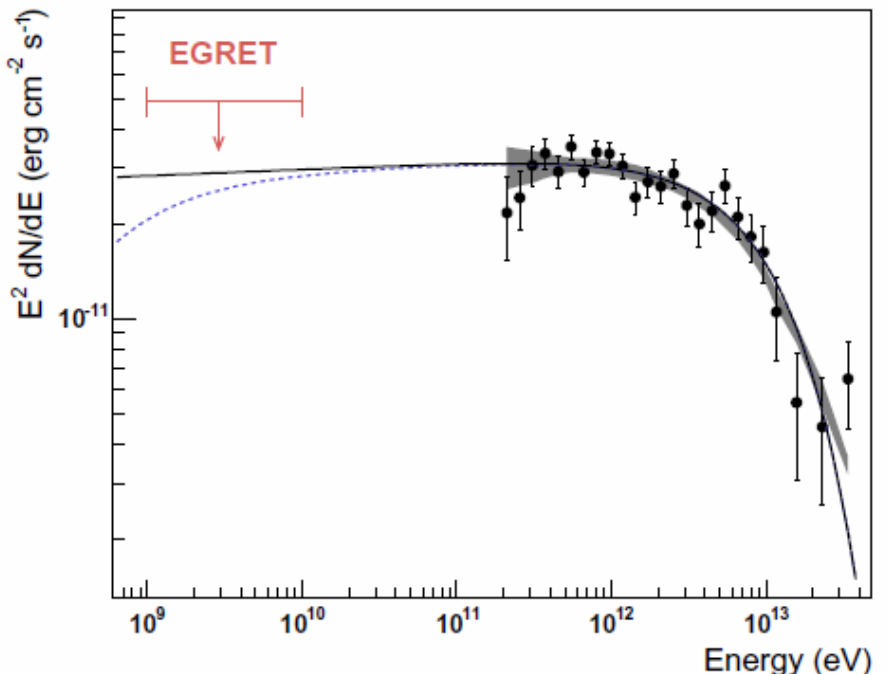


**Fig. 20.** H.E.S.S. data points plotted in an energy flux diagram. They shaded grey band is the systematic error band for this measurement (see Sect. 3.2). The black curve is the best fit of a power law with exponential cutoff to the data, extrapolated to lower energies. The dashed blue curves is the same function, but it takes the  $\pi^0$  kinematics into account. The EGRET upper limit from 1 GeV to 10 GeV is plotted as red arrow.

⇒ Protons favored (?)

# Spectral variation: not seen

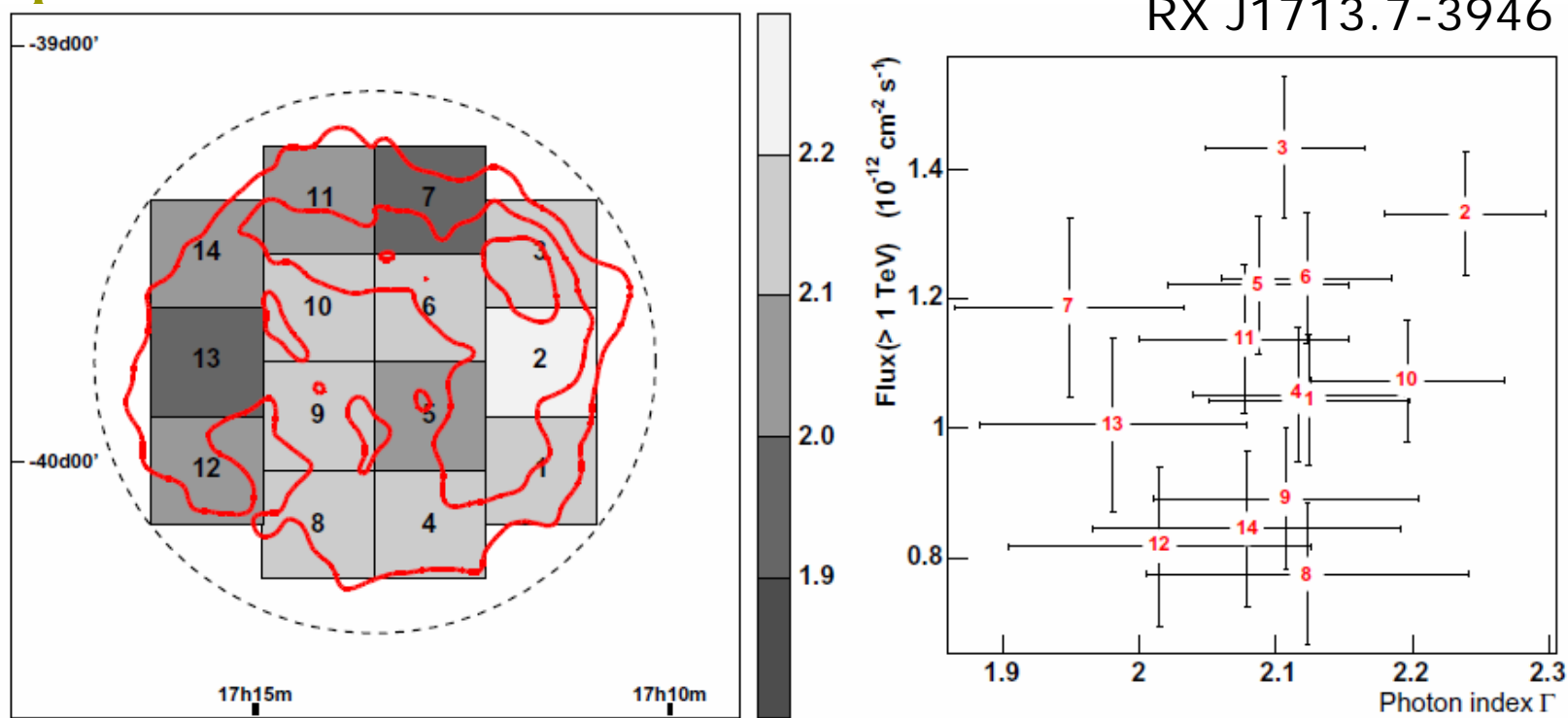
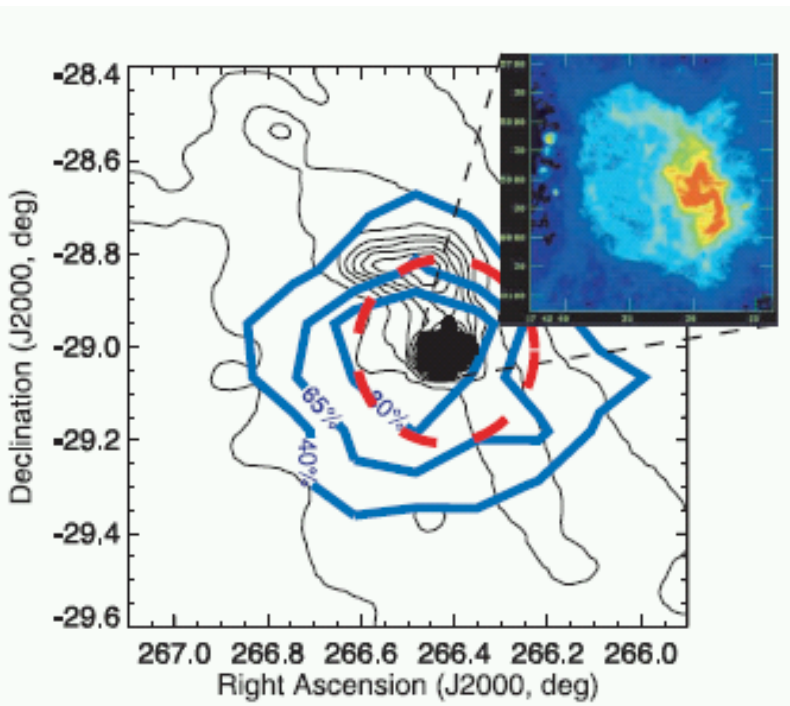
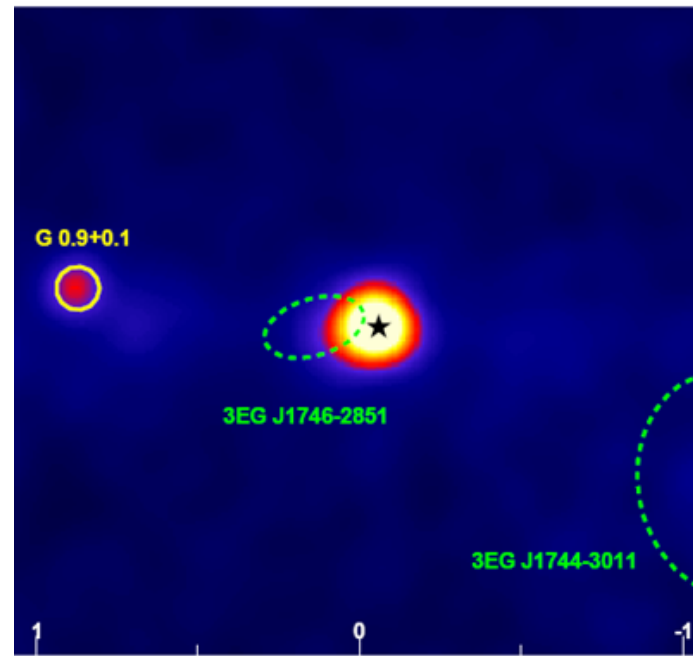


**Fig. 14.** The image illustrates the results of the spatially resolved spectral analysis. **Left part:** Shown in red are gamma-ray excess contours from Fig. 7, linearly spaced at 30, 60, and 90 counts. Superimposed are the 14 boxes (each  $0.26^\circ \times 0.26^\circ$  in dimension) for which spectra were obtained independently. The dashed line is the  $0.65^\circ$  radius circle that was used to integrate events to produce a spectrum of the whole SNR. The photon index obtained from a power-law fit in each region is colour coded in bins of 0.1. The ranges of the fits to the spectra have been restricted to a maximum of 8 TeV (see Table 2). **Right part:** Plotted is the integral flux above 1 TeV against the photon index, for the 14 regions the SNR was sub-divided in. The error bars are  $\pm 1\sigma$  statistical errors. Note that systematic errors of 25% on the flux and 0.1 on the photon index are to be assigned to each data point additionally.

# Galactic Center/Sgr A\*



CANGAROO-II (Tsuchiya  
et al., ApJ 606, L115, 2004)



H.E.S.S.: W.Hofmann,  
ICRC2005

# Dark matter signal from Sgr A\*?

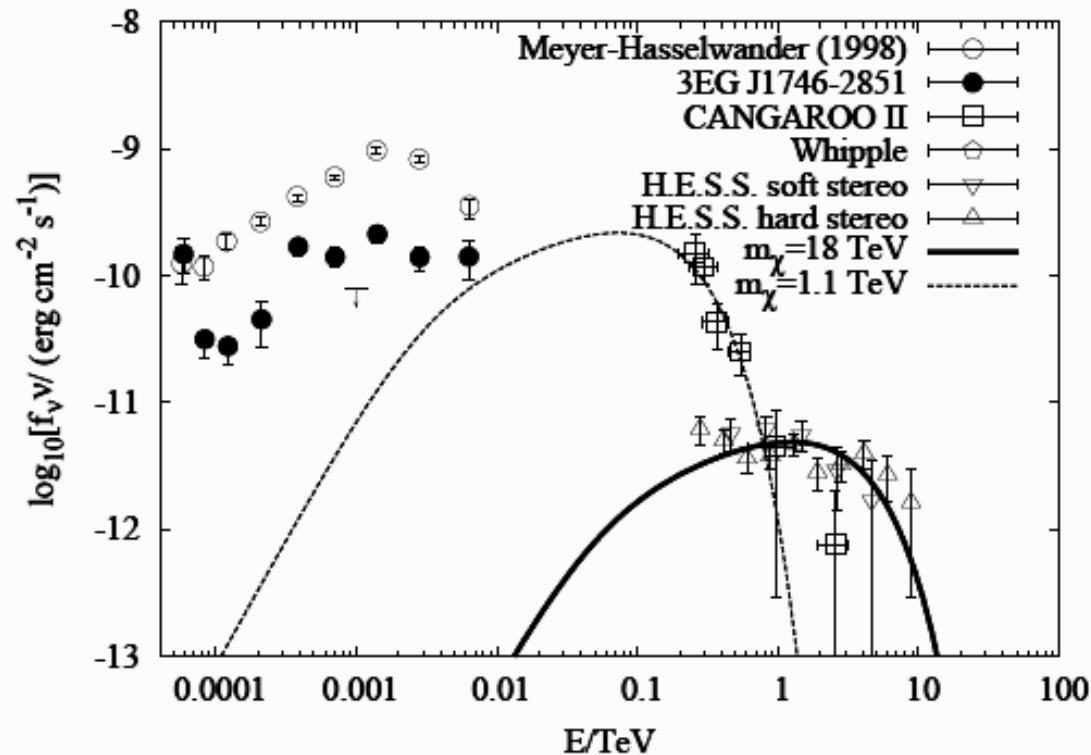
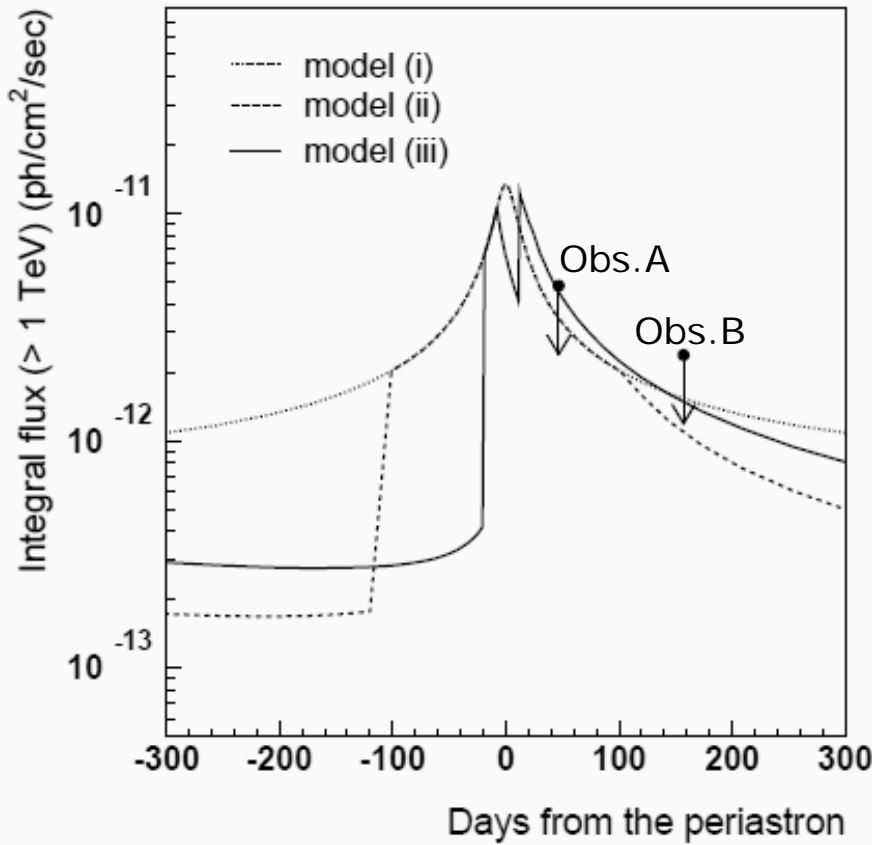
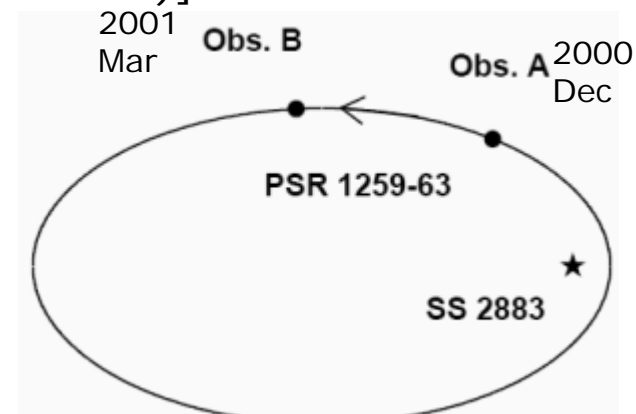


Fig. 2. A summary of data and best-fit models for WIMP annihilation from the Galactic center: H.E.S.S. (open triangles), CANGAROO (open boxes), EGRET (solid and open circles), 10m Whipple telescope of the VERITAS collaboration (solid diamond).

# PSR 1259-63/SS2883



- (i) aligned disc to the orbital plane and interaction throughout the orbit
- (ii) mis-aligned disc and interaction in the  $\sim 200$ -day period around periastron ( $\tau$ ), during which the radio emission is depolarized
- (iii) mis-aligned disc and interaction in two short periods,  $[(\tau - 18 \text{ d}) \sim (\tau + 8 \text{ d})]$  and  $[(\tau + 12 \text{ d}) \sim (\tau + 22 \text{ d})]$



# SNR RX J0852.0-4622 (G266.2-1.2, Vela Jr.)

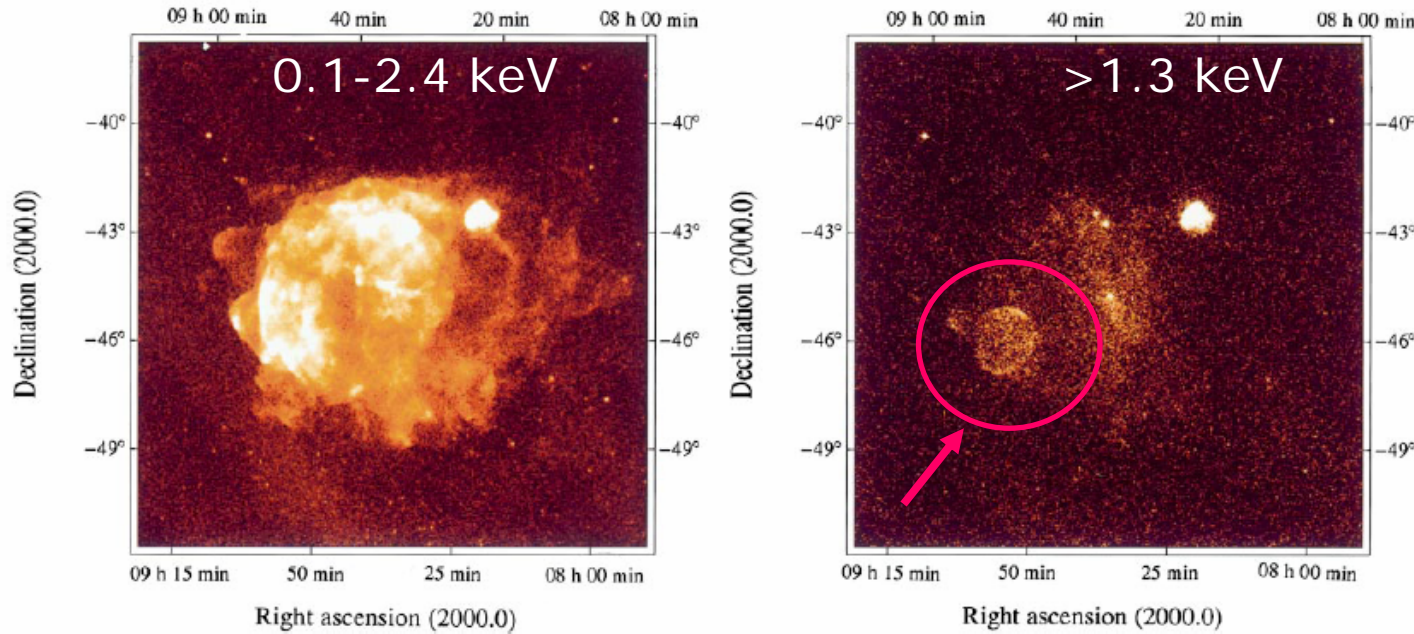
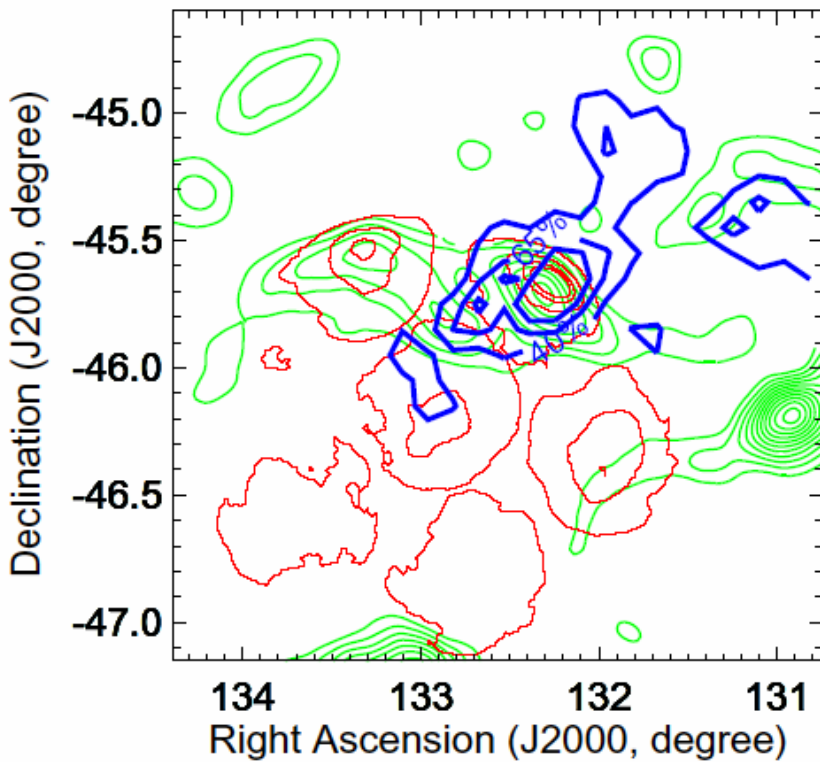


**Figure 1** Rosat all-sky survey images of the Vela SNR and its surroundings. Angular resolution is 1 arcmin half-power radius; mean exposure is 993 s. The left-hand image was taken for photon energies  $0.1 < E < 2.4$  keV; surface brightness increases from dark yellow to white by a factor of 500. The right-hand image is for photon energies  $>1.3$  keV. Most of the Vela SNR X-ray emission which dominates at low energies had disappeared. At the centre, the synchrotron nebula around the Vela pulsar remains visible as well as the SSW beam-like structure, and at the very northwest (upper right) the bright Puppis-A SNR can be seen. The new shell-type SNR RX J0852.0 – 4622 shows up in the lower left. East of RX J0852.0 – 4622 hard X-ray photons from the D/D' Vela SNR shrapnels are seen which, however, are associated with a much lower-temperature spectrum than RX J0852.0 – 4622 (ref. 14). For X-ray spectral analysis, RX J0852.0 – 4622 was divided into two

regions, one containing the bright northern limb section (l) and the other one (r) excluding the northern and southern limbs. Spectral fits were performed with either power-law models, optically thin thermal emission equilibrium models (Raymond-Smith models) or combinations of both. Solutions with a reduced  $\chi^2 < 1$  for region r are obtained only with a two-temperature model with  $kT_{t,1} = 0.14^{+0.08}_{-0.08}$  keV,  $kT_{t,2} = 2.5^{+4.5}_{-0.7}$  keV. The spectrum of the northern limb can be fitted by either a simple power law with index  $\alpha = -2.6^{+0.3}_{-0.4}$  or a two-temperature model with  $kT_{l,1} = 0.21^{+0.14}_{-0.09}$  keV,  $kT_{l,2} = 4.7^{+4.5}_{-0.7}$  keV. The presence of low-temperature components may partially be due to a residual, uncorrected contribution from the much softer Vela SNR. The total, absorption-corrected flux of the high-temperature components is  $F_x(0.1-2.4 \text{ keV}) = 3 \times 10^{-10} \text{ erg cm}^{-2} \text{ s}^{-1}$ .

# SNR RX J0852.0-4622



CANGAROO-II: Katagiri et al.,  
ApJ, 619, (2005) L163

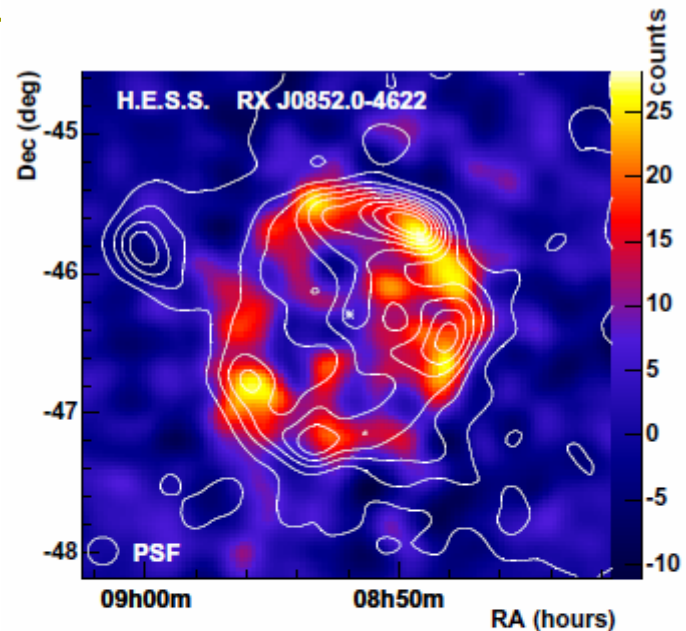


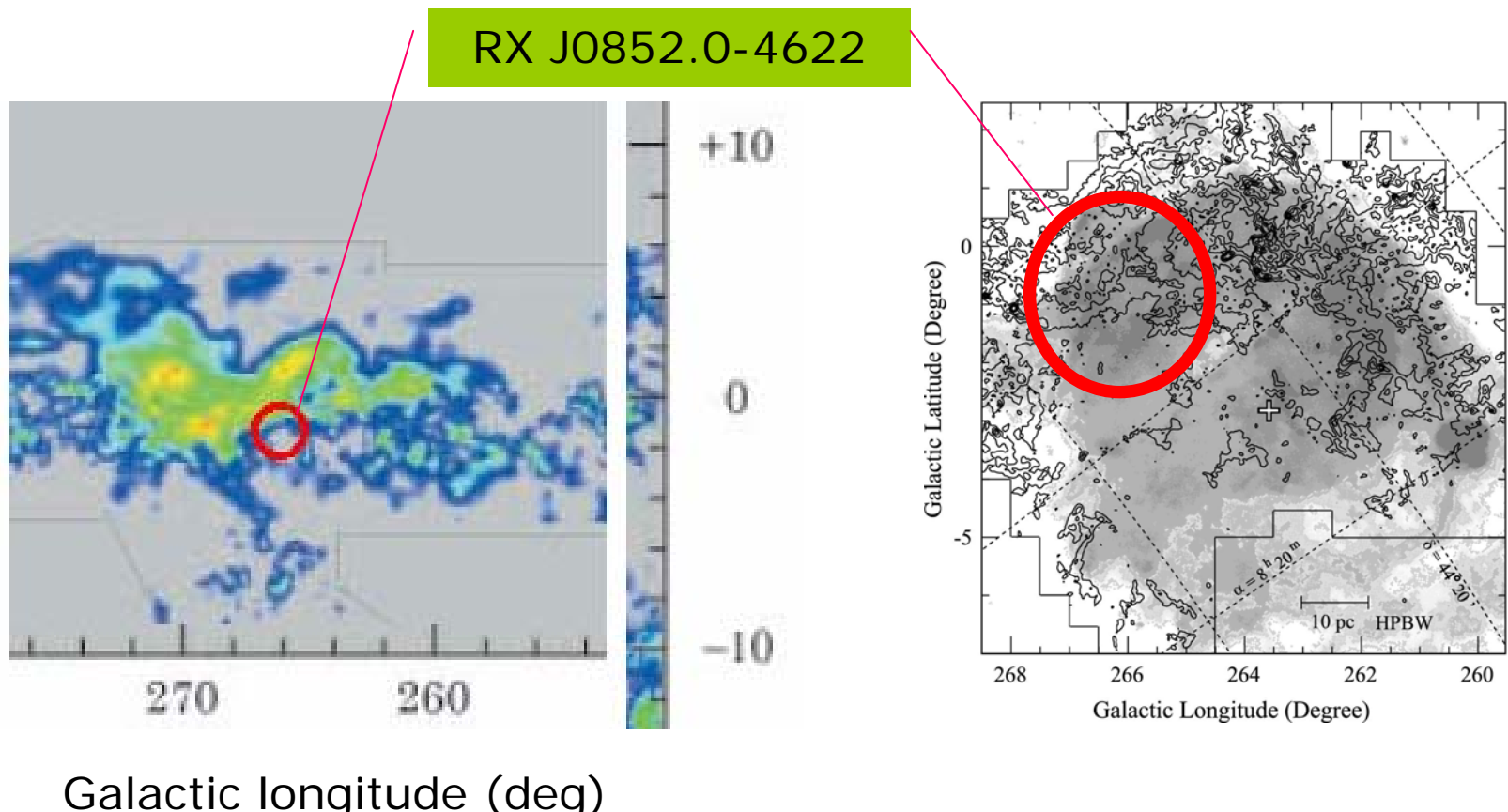
Fig. 2. Count map of  $\gamma$ -rays from the direction of RX J0852.0-4622 after background subtraction. The data are smoothed with a Gaussian ( $\sigma = 0.1^\circ$ ) representing the angular resolution of the instrument. The point spread function (PSF) is indicated by a circle.  $\gamma$ -ray features smaller than the PSF should not be considered as real. The lines denote equidistant contours of smoothed ( $\sigma = 0.1^\circ$ ) X-ray data from the ROSAT All Sky Survey, with energies restricted to above 1.3 keV. The position of the neutron star candidate AX J0851.9-4617.4 is marked with an asterisk. The axes show J2000.0 equatorial coordinates.

H.E.S.S.: Aharonian et al., AA  
437, L7 (2005)

# Correlation with CO

Dame et al., ApJ 547, 792 (2001)

Moriguchi et al., PASJ 53, 1025 (2001)



→ Need detailed study

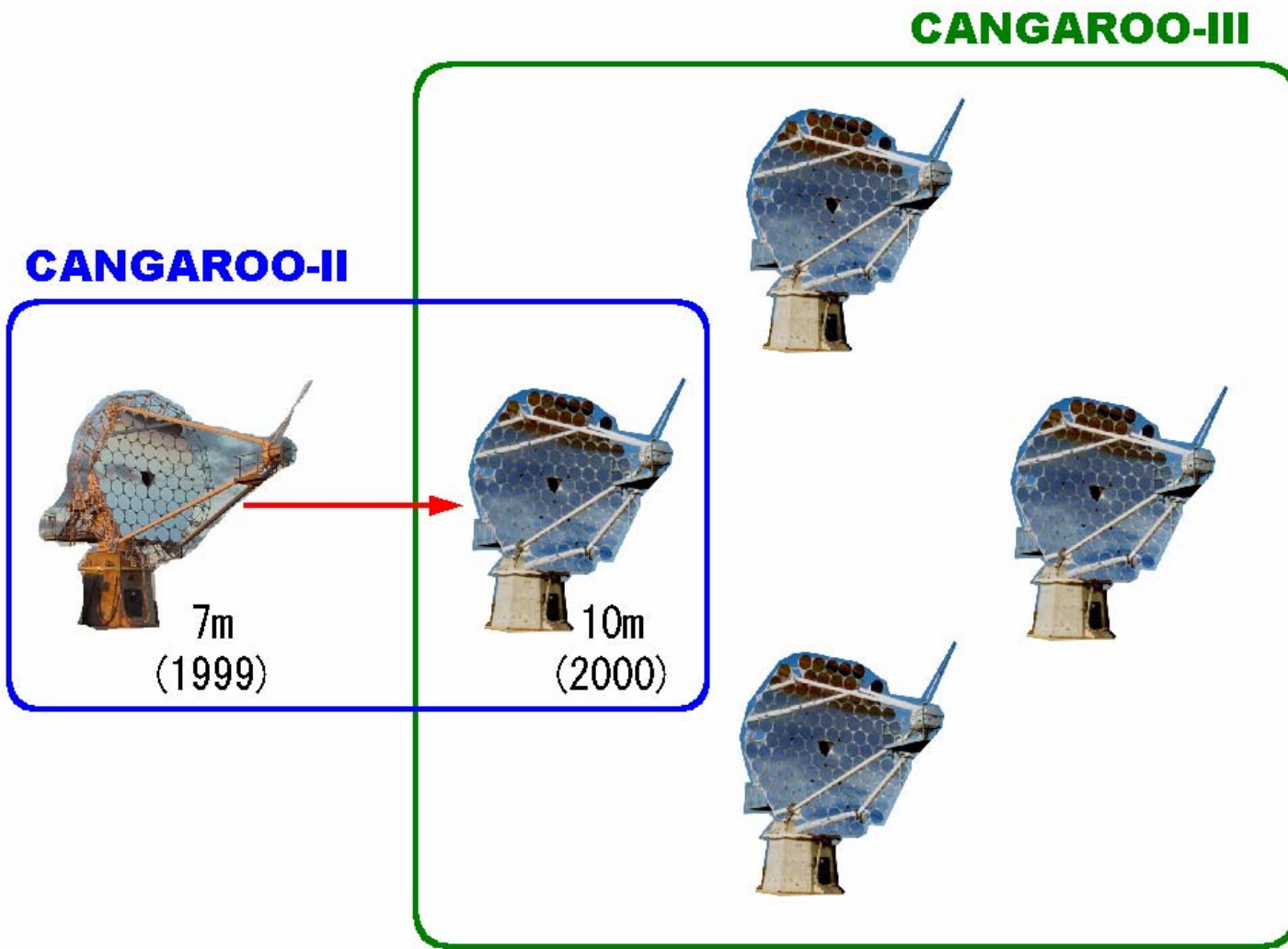
# CANGAROO-II results: summary

---

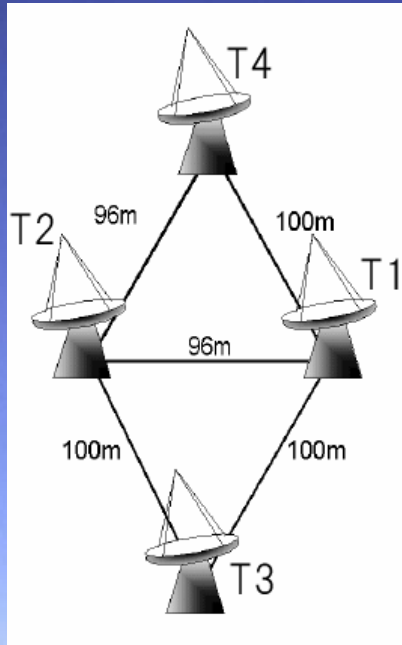
	Signal	Publish	H.E.S.S.
□ SNR RX J1713.7-3946	○	Nature'02	○
□ Blazar Mrk421	○	ApJL'02	○
□ Starburst galaxy NGC253	○	A&AL'03	↓
□ SNR SN1987A	↓	ApJL'03	↓
□ Galactic Center	○	ApJL'04	○
□ Pulsar binary PSR 1259-63/SS2883	↓	ApJ'04	○v
□ SNR RX J0852.0-4622 (Vela Jr.)	○	ApJL'05	○

Signal: ○ detected, ↓ upper limit, v: variable

# CANGAROO-II & -III



# CANGAROO-III: 2004 March



# Basic specifications of telescopes

## □ Location:

- $31^{\circ}06'S, 136^{\circ}47'E$
- 160m a.s.l.

## □ Telescope:

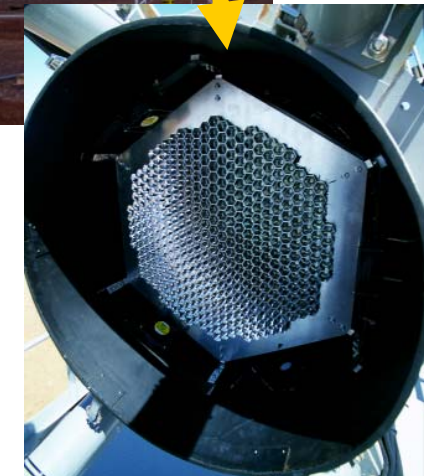
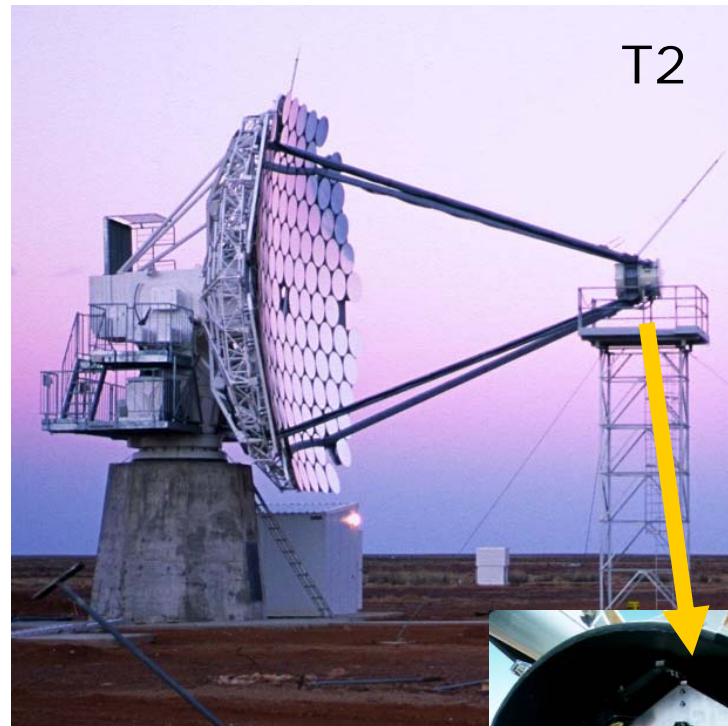
- $114 \times 80\text{cm}\phi$  FRP mirrors  
( $57\text{m}^2$ , Al surface)
- 8m focal length
- Alt-azimuth mount

## □ Camera:

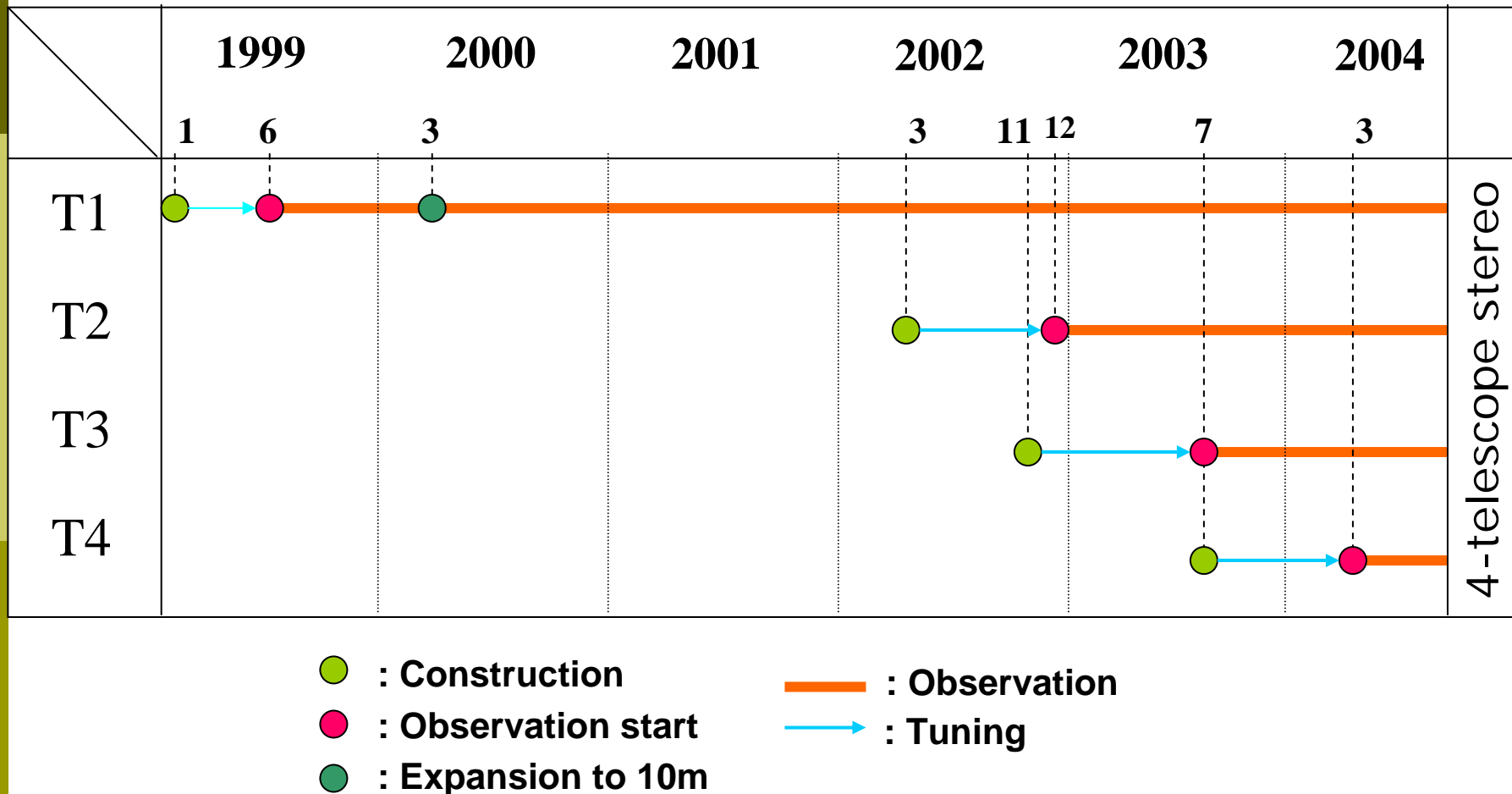
- T1: 552ch ( $2.7^{\circ}$  FOV)
- T2,T3,T4: 427ch ( $4^{\circ}$  FOV)

## □ Electronics:

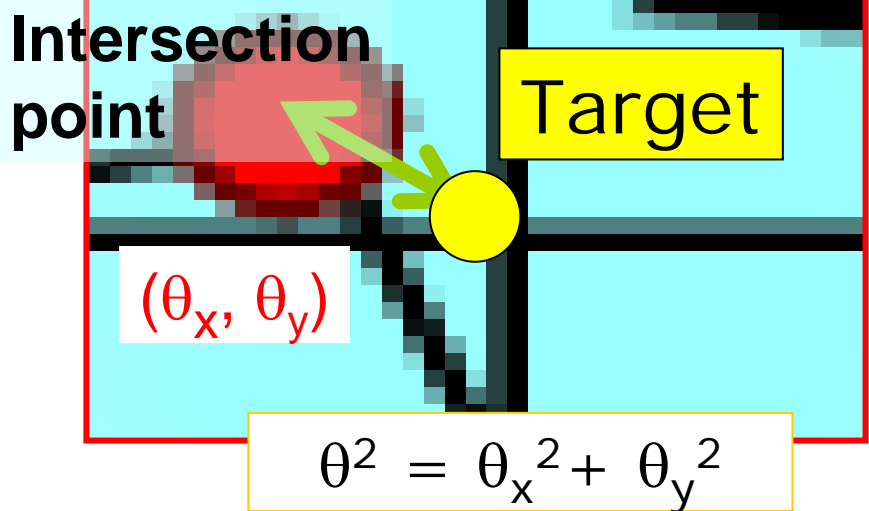
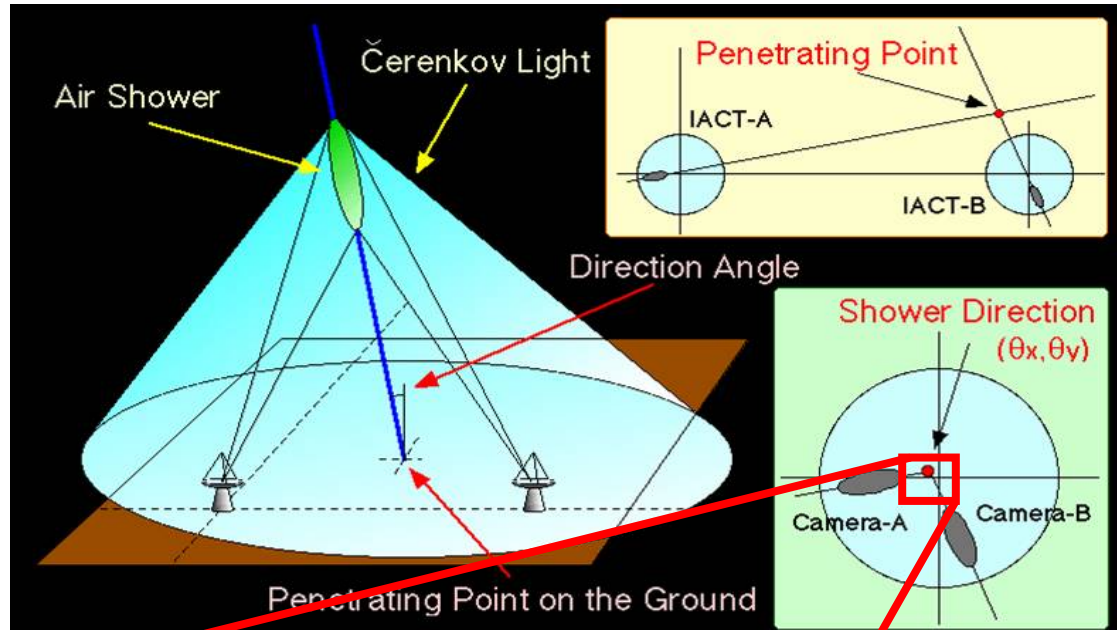
- TDC+ADC



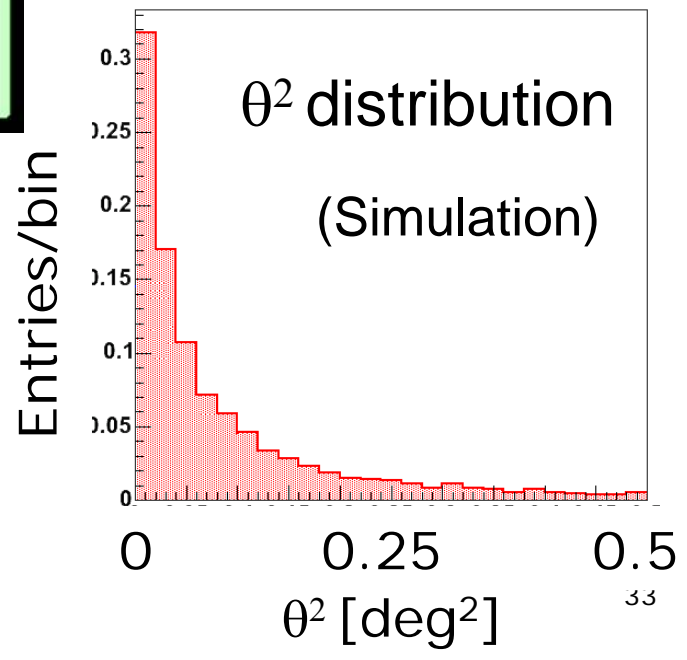
# Construction of CANGAROO-III



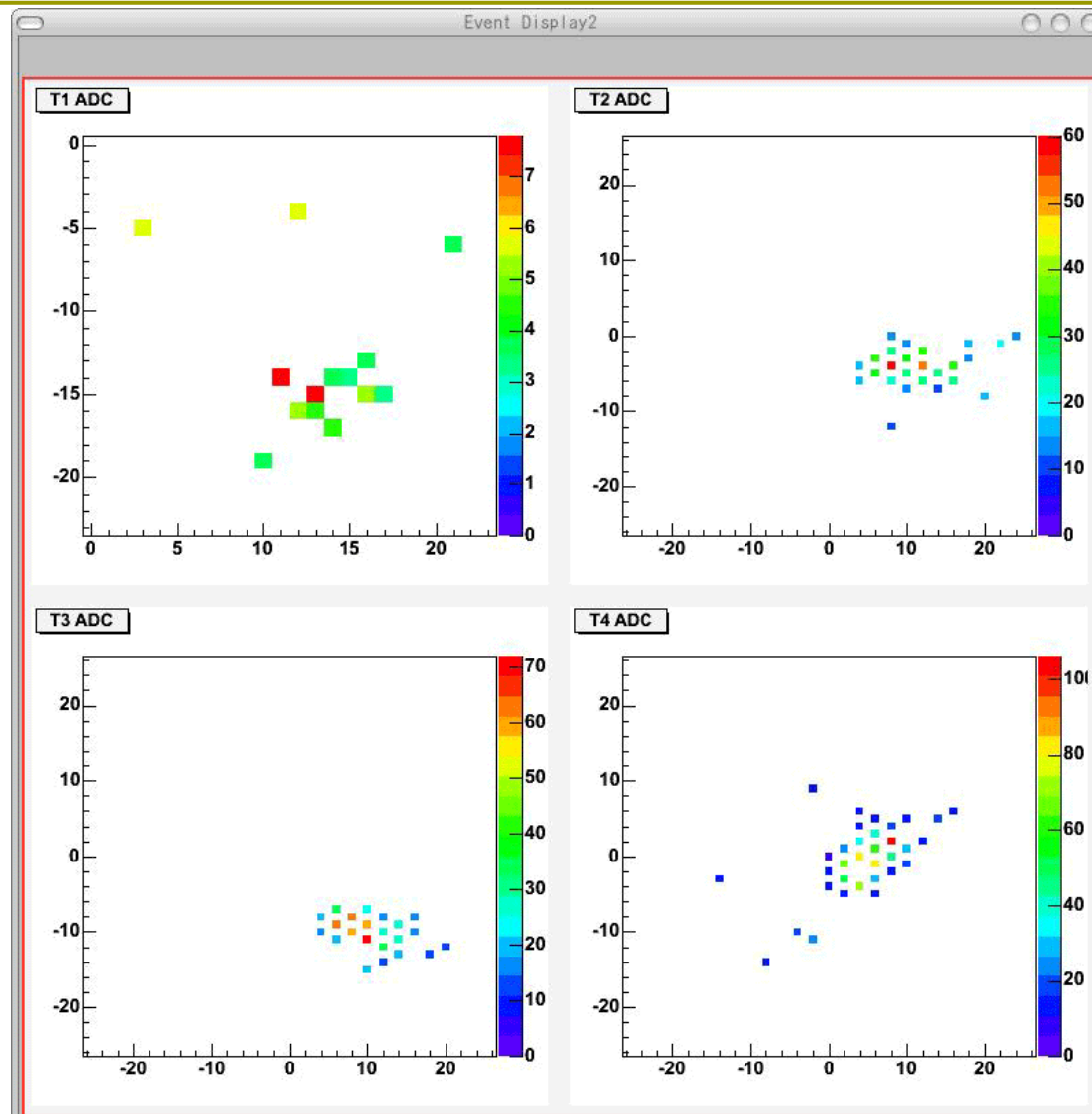
# Stereo observation



Angular resolution  
0.25deg → 0.1 deg  
Energy resolution  
30% → 15%  
Better S/N (no local muons)



# Sample of 4-fold stereo events



Data:  
2004  
March

# Stereo analysis: in progress

---

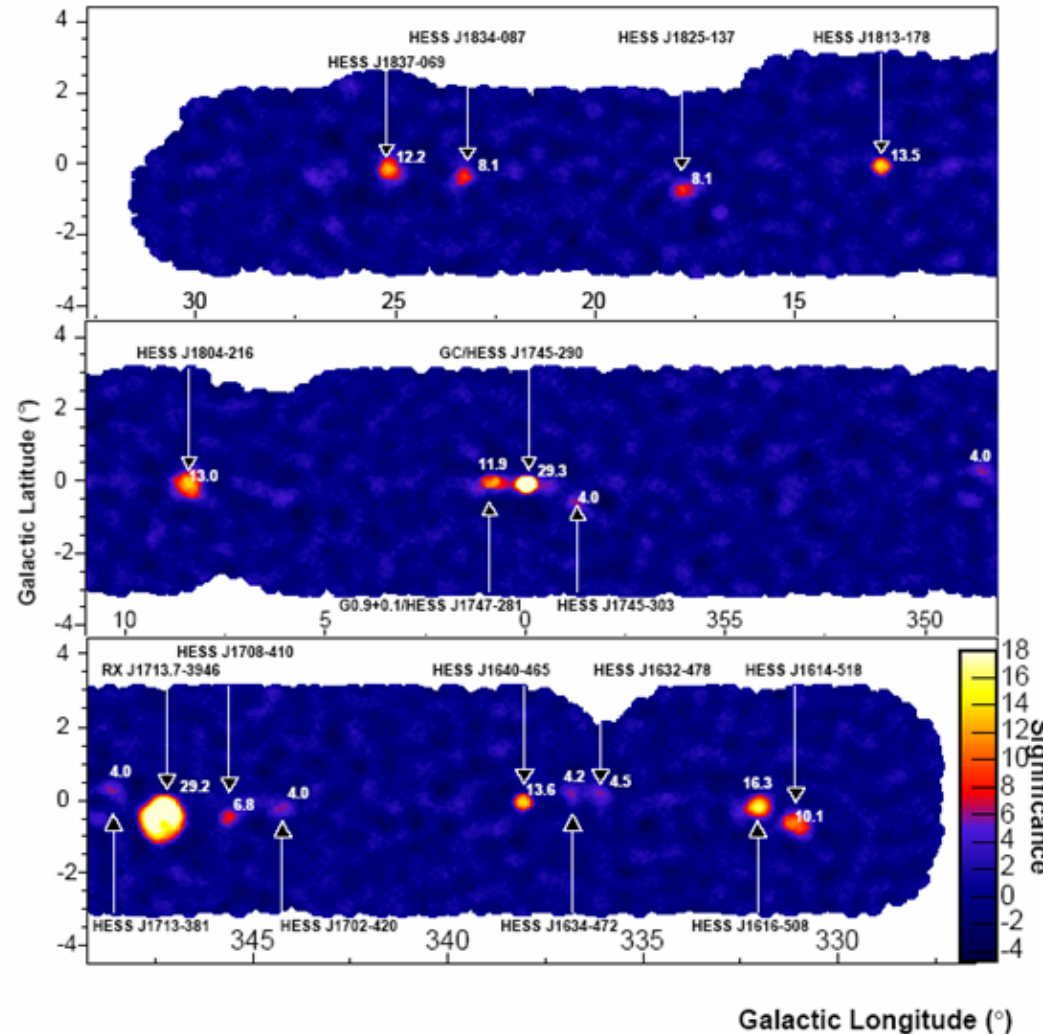
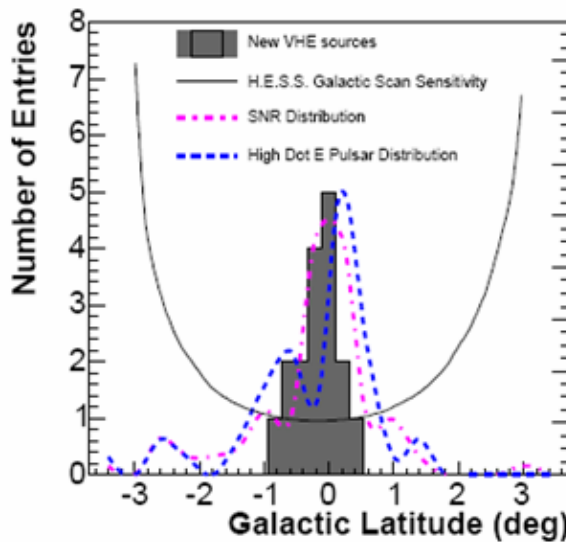
- Inconsistency with H.E.S.S results on some sources  
⇒ New observations with CANGAROO III  
Efforts for advanced analysis procedures
- Measure more optical parameters
  - CCD measurements of spotsizes and stars
- Use muons for calibration
  - Tune Monte Carlo simulation
- Use the Crab as the standard candle
  - Flux obtained with Monte Carlo simulation is compared with those reported by other groups
- Independent teams within the collaboration are working:
  - Results, especially detections, are double-checked

# H.E.S.S. Highlight: Galactic Plane Survey

- S. Funk, OG 23
- A. Lemiere, OG 23

15 new TeV sources  
+ 3 known

Scale height:  
 $\approx 0.3^\circ$  rms  
 $\approx$  molecular gas

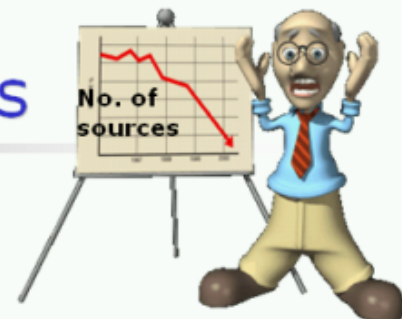


# H.E.S.S. results

W.Hofmann, Cherenkov2005

## H.E.S.S. and the “known” sources

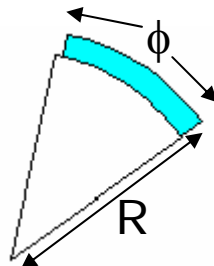
Southern hemisphere TeV sources



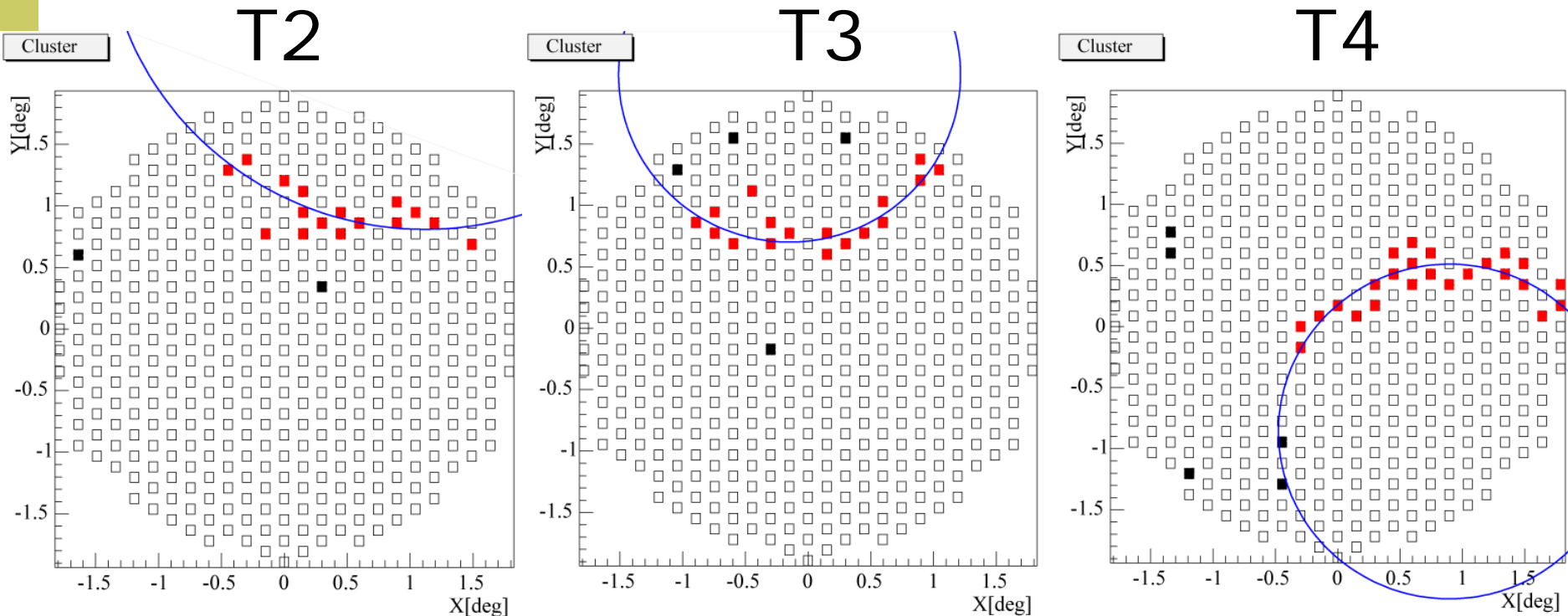
Object	Current status
PSR 1706-44	H.E.S.S.: limit well below old flux <small>A&amp;A</small>
Vela pulsar	H.E.S.S.: limit well below old flux
SN 1006	H.E.S.S.: limit well below old flux <small>A&amp;A in press</small>
NGC 253	H.E.S.S.: limit well below old flux <small>to be subm.</small>
Gal. center	H.E.S.S.: $>30\sigma$ , spectrum differs <small>A&amp;A</small>
RX J1713	H.E.S.S.: $>30\sigma$ , spectrum & flux similar <small>Nature</small>
PKS 2155	H.E.S.S.: $>100\sigma$ , variable source <small>A&amp;A</small>

# Muon events (1)

- Selected by
  - 1) clustering
  - 2)  $R \times \phi$  (arc length)  $> 2\text{deg} \cdot \text{rad}$
  - 3) Small  $\chi^2$  (good fit)

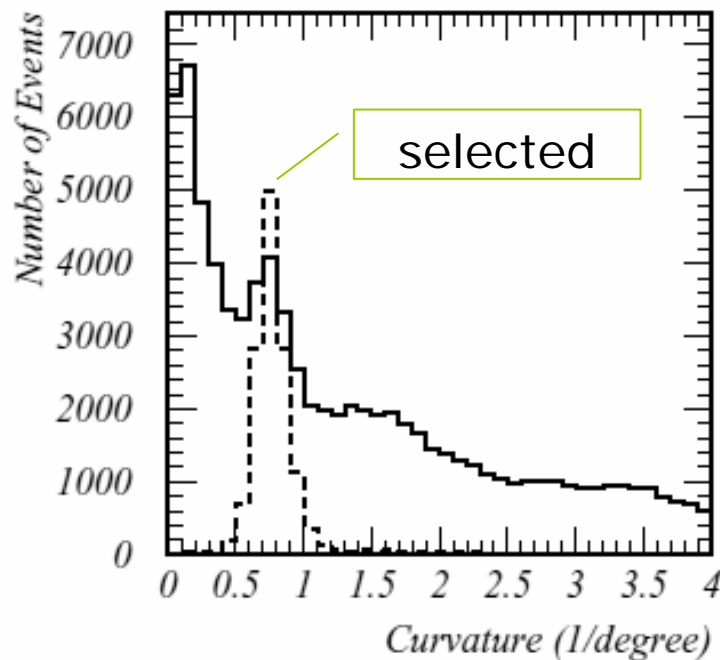


Data: 2004 March



# Muon events (2)

---

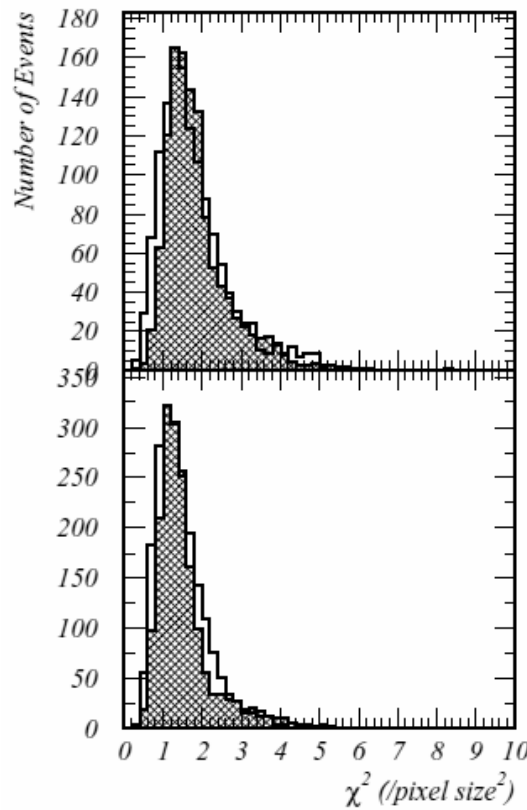


Local muons:  
Cherenkov angle  $\sim 1.3^\circ$   
or  
Curvature  $\sim 1/1.3^\circ$

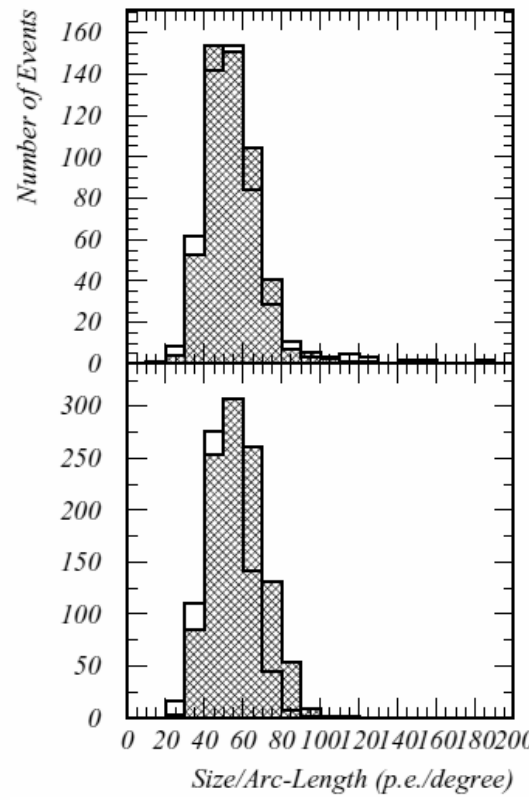
FIG. 2.— Curvature distribution for the circular fitting results of all events for T3. The solid histogram is for all events and the dashed one for the selected events (with the vertical scale multiplied by 5).

# Muon parameters compared with Monte Carlo

T2



T3

 $\chi^2$ 

size/arclength

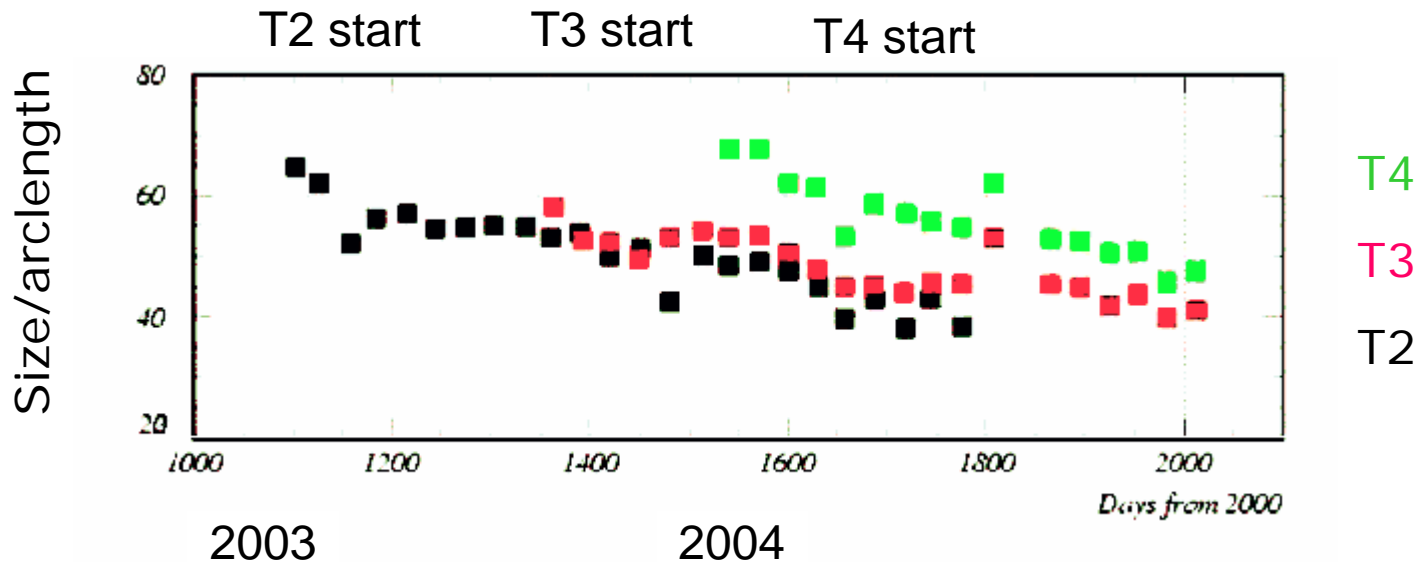
Histogram: data

Hatched: M.C.

$\chi^2$ : for ring fitting  
(sensitive to spot size)

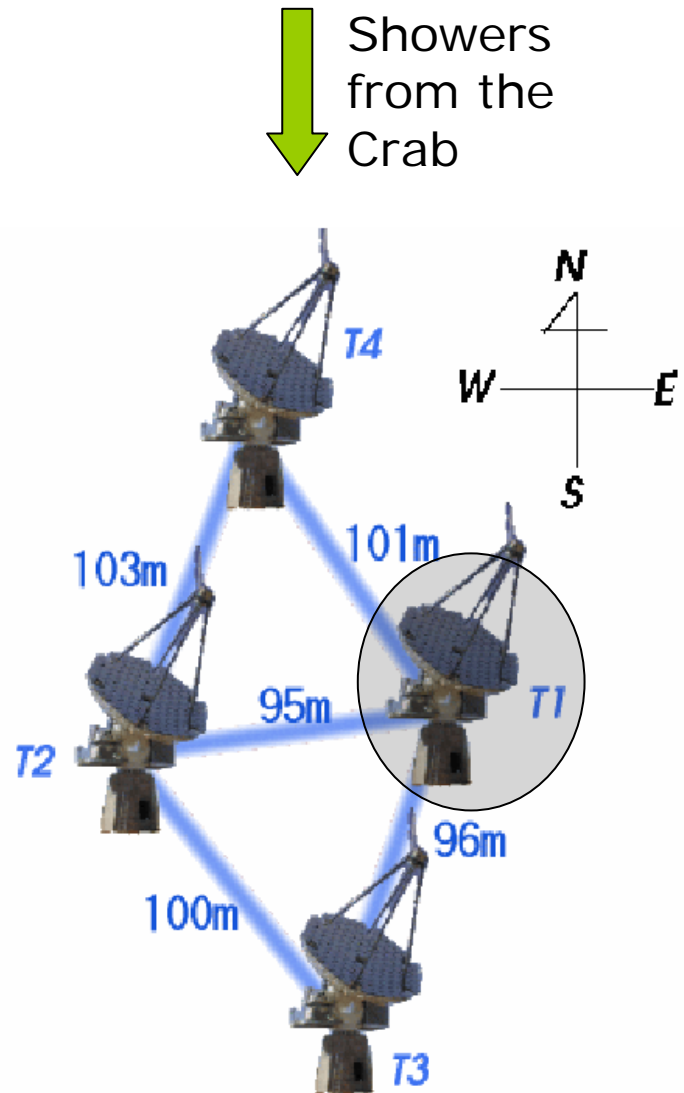
Size/arclength  $\propto$   
total light collection  
efficiency

# Time variation of Size/Arclength



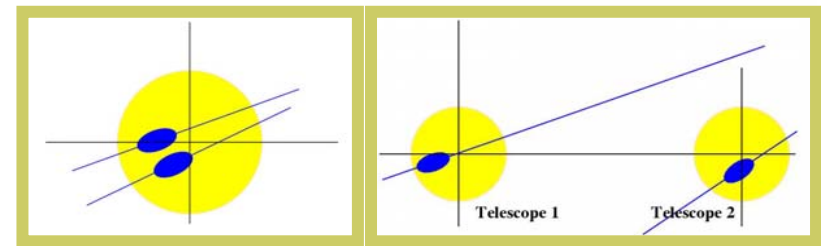
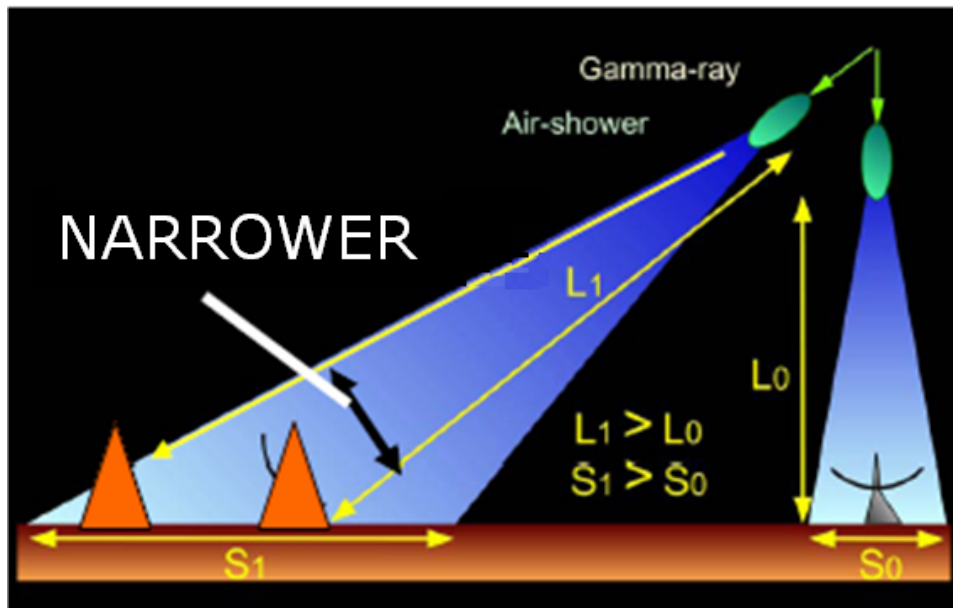
- Monitor of total light conversion efficiency
- Gradually, *Size/Arclength* is decreasing (~5% / year)
- Mirror degradation due to dust etc.

# Unfortunate situation for the Crab



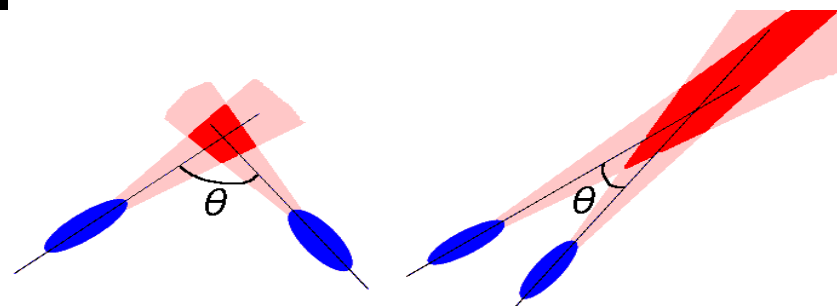
- The oldest T1 has higher energy threshold and bad efficiency for stereo observation
- Only T2/T3/T4 are used for stereo analysis
- Stereo baseline becomes short for the Crab observation at large zenith angles

# Large zenith angle observation of the Crab



Higher energy threshold  $\sim 1\text{TeV}$

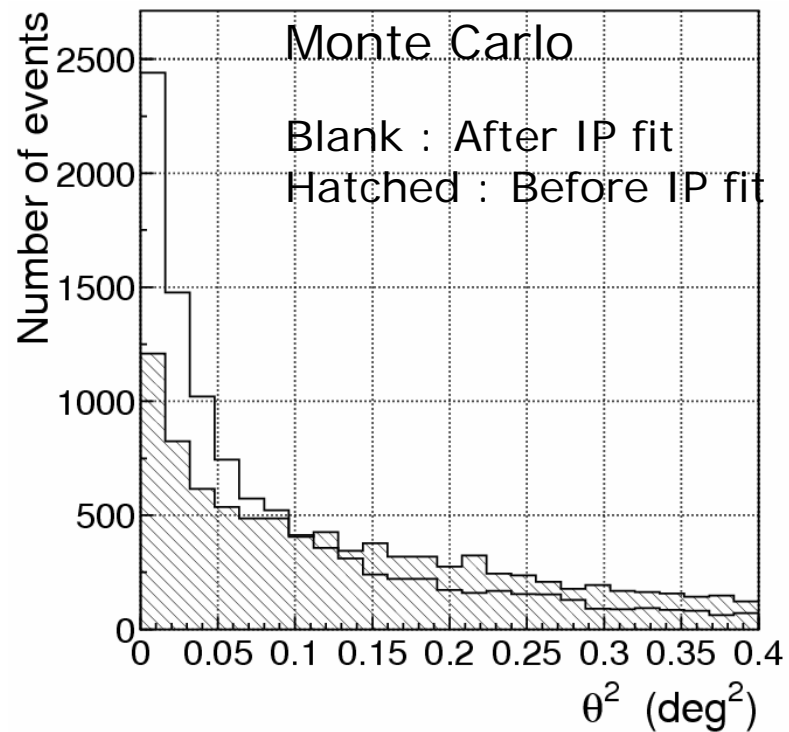
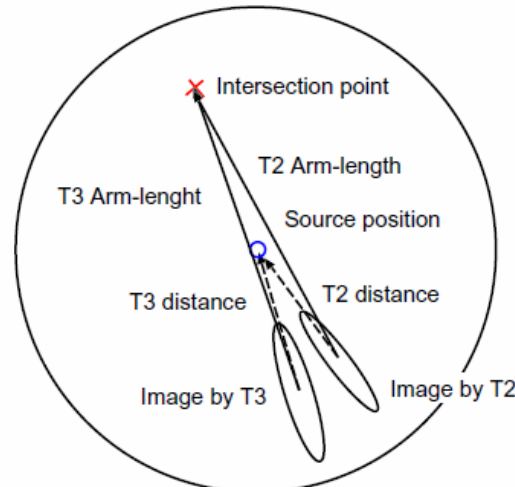
Bad intersection accuracy



# IP constraint fit

$$\chi^2 \equiv \sum_{\text{Telescopes}} \left[ \left( \frac{\text{Width}(x,y)}{\sigma_w} \right)^2 + \left( \frac{\text{Armlength}(x,y) - \langle \text{Armlength} \rangle}{\sigma_{ARM}} \right)^2 \right]$$

Search intersection point (IP) by minimizing  $\chi^2$  so that width along shower axis to be minimum and armlength to be near the expected value ( $\langle \text{Armlength} \rangle = 0.75$ , Mesh size  $0.025^\circ$ )



# $\gamma/h$ separation by Fisher discriminant

- Linear combination of image parameters ( $x_i$ )

$$F \equiv \sum_i \alpha_i x_i$$

- Difference between signal ( $\gamma$ ) and background ( $h$ )

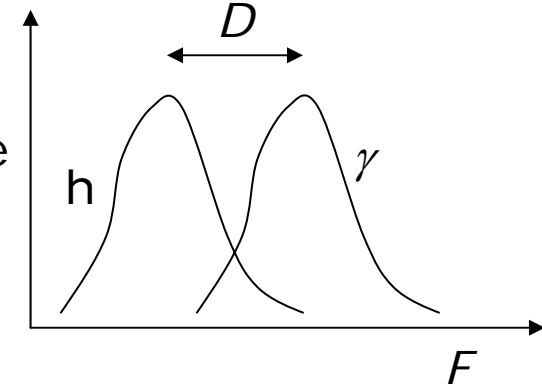
$$D \equiv \langle F_\gamma \rangle - \langle F_h \rangle$$

- Determine  $\alpha_i$  which maximize separation (solvable using correlation matrix)

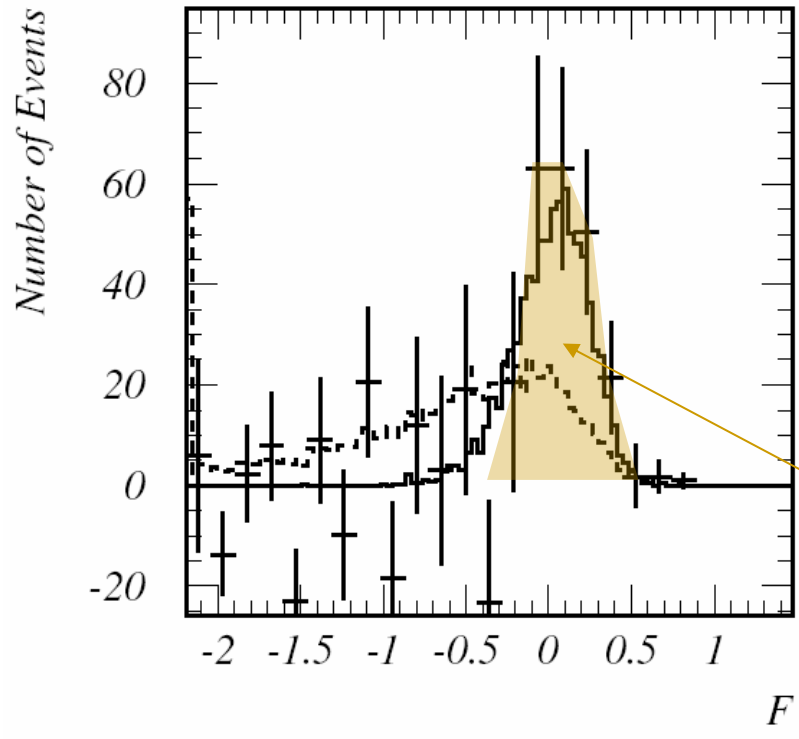
$$S \equiv \langle D \rangle^2 / \langle (D - \langle D \rangle)^2 \rangle$$

- With calculated  $\alpha_i$ , for a known source, the (appropriately normalized) combination  $F$  could be the “Fisher discriminant” for other sources.

- We use *widths* and *lengths* of multiple telescopes for image parameters.

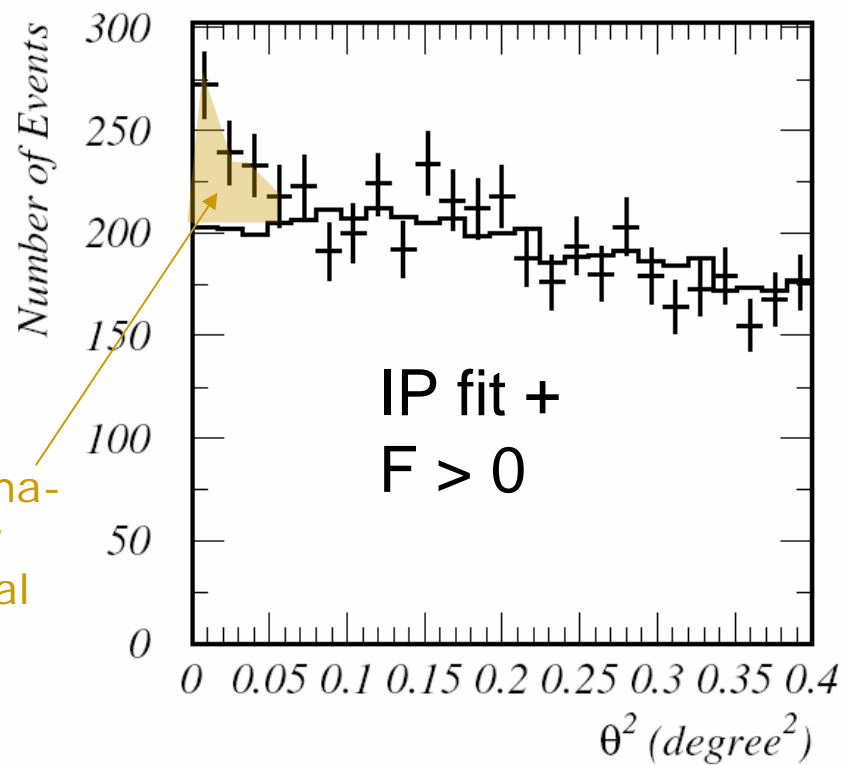


# Crab signal



Plot : observation  
 Solid : MC gamma  
 Dashed : background

- T2 & T3
- 890 min (Dec. 2003)



203 excess events  
 5.8 sigma

# Crab spectrum

---

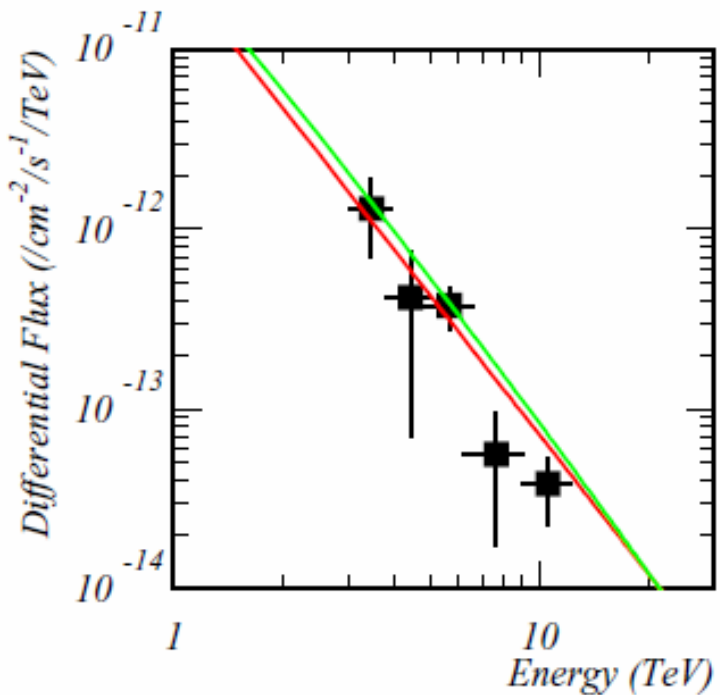
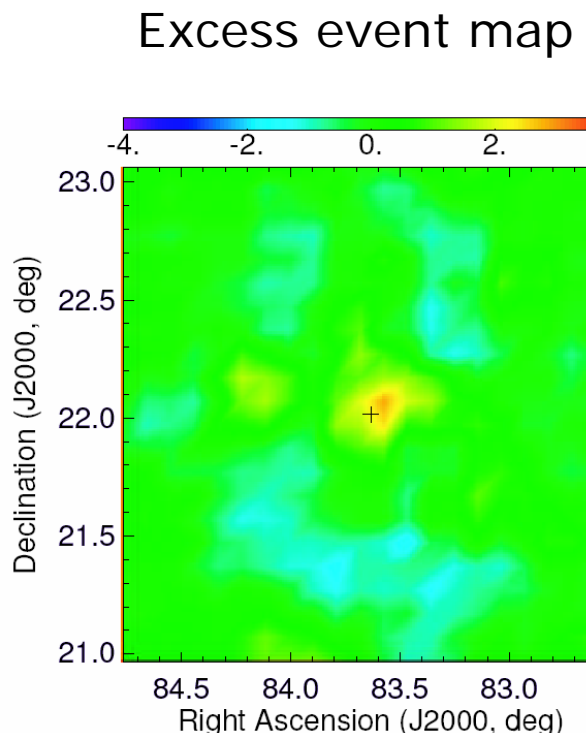


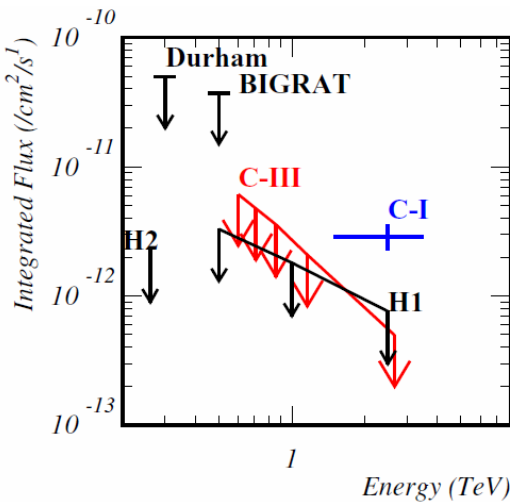
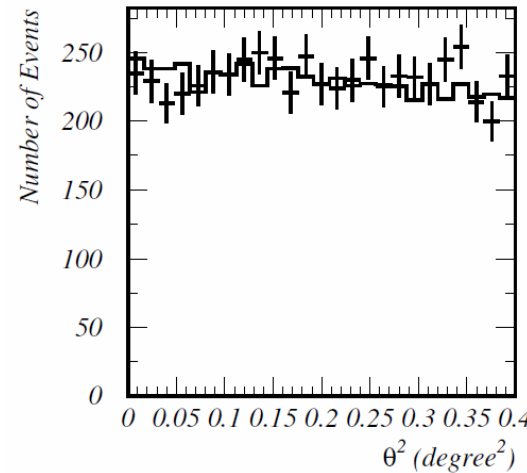
FIG. 17.— Differential gamma-ray flux from the Crab Nebula as a function of energy. The red line is the HEGRA result (Aharonian et al. 2000) and the green is the Whipple result (Hillas et al. 1998).



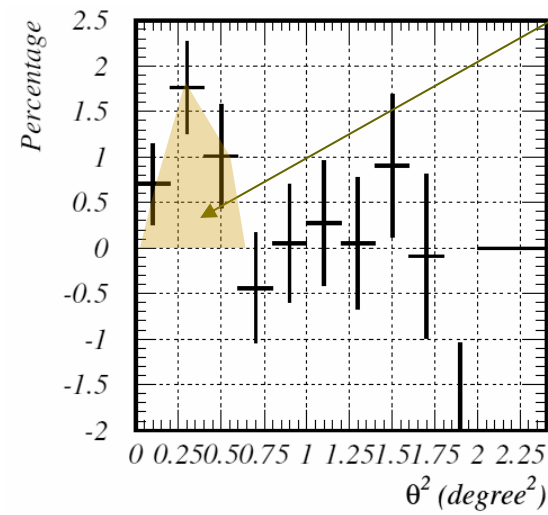
Angular resolution  $\sim 0.23 \text{ deg}$

# Vela pulsar/nebula

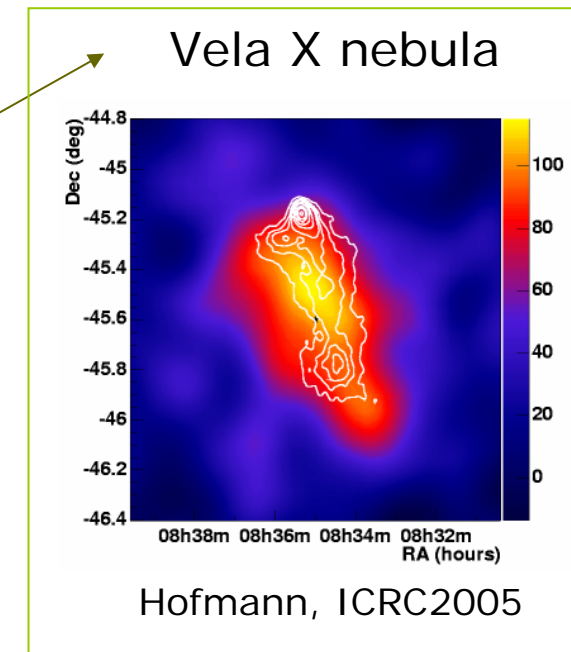
## Pulsar position



- Pulsar pointing (2004 Jan/Feb)
- T2 & T3 wobble, 1,311 min.
- Fisher discriminant



$\theta^2$  from Vela X center



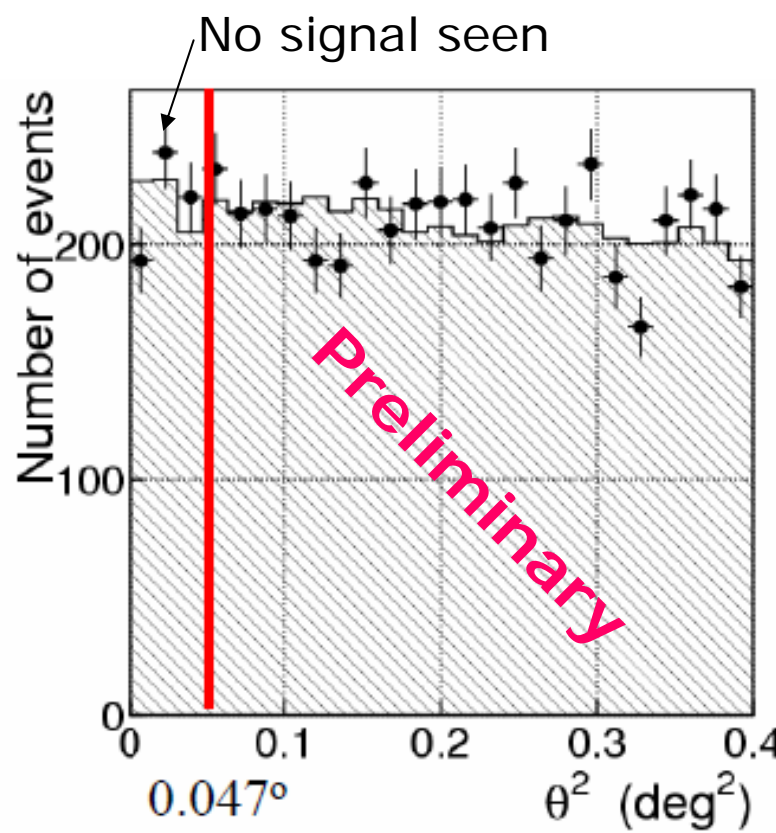
# Cen A: the nearest AGN

S. Kabuki



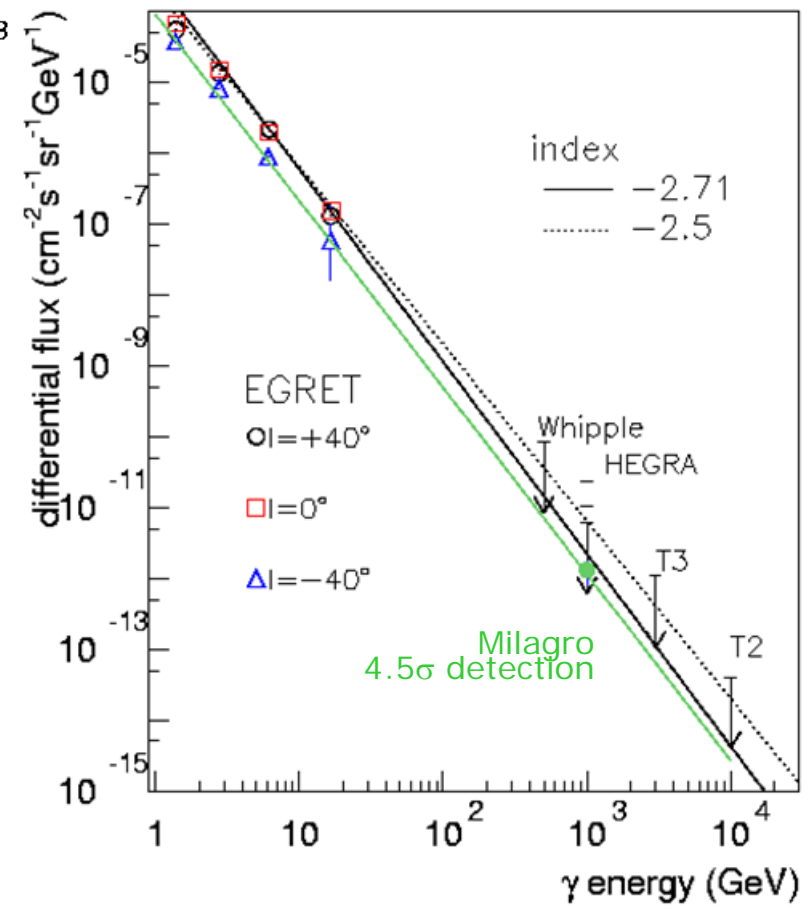
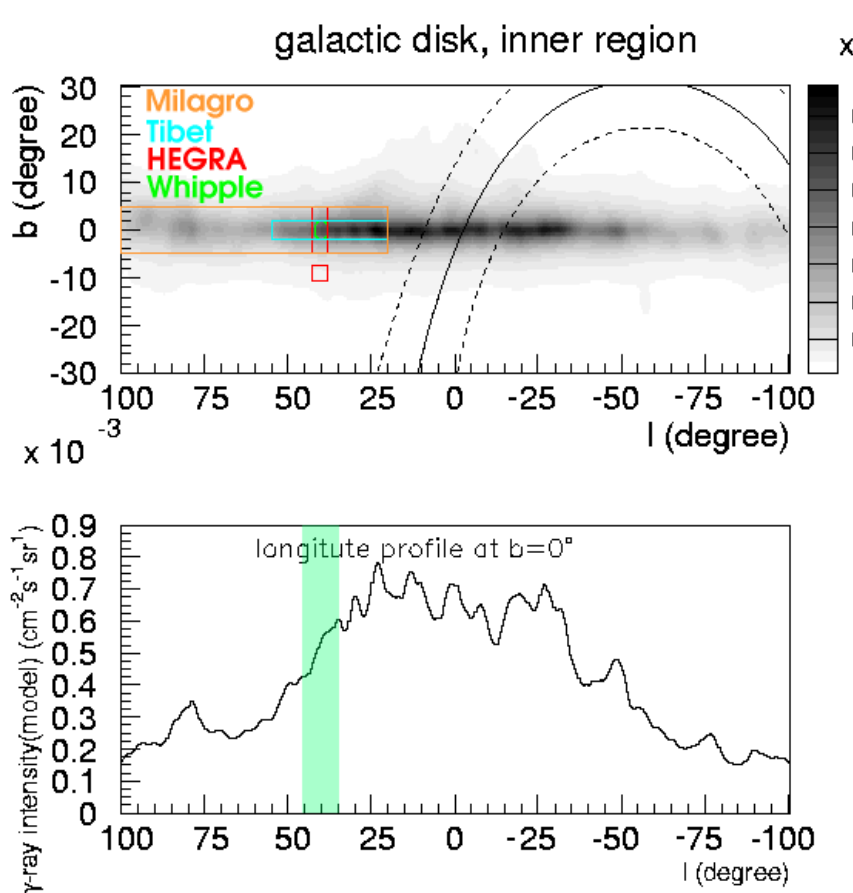
Near infrared image  
2MASS  
 $1.2\text{-}2.17\mu\text{m}$

- Elliptical
- Radio galaxy
- Fanaroff-Riley type I
- “Misaligned” BL Lac ( $\sim 60^\circ$ )
- Distance 3.5 Mpc ( $z=0.00183$ )



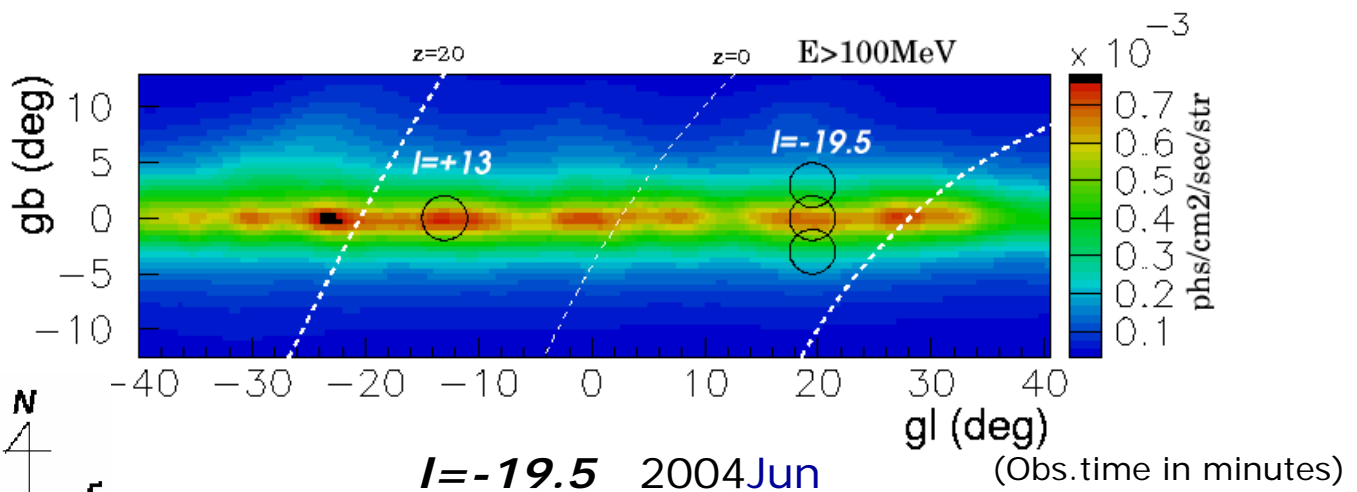
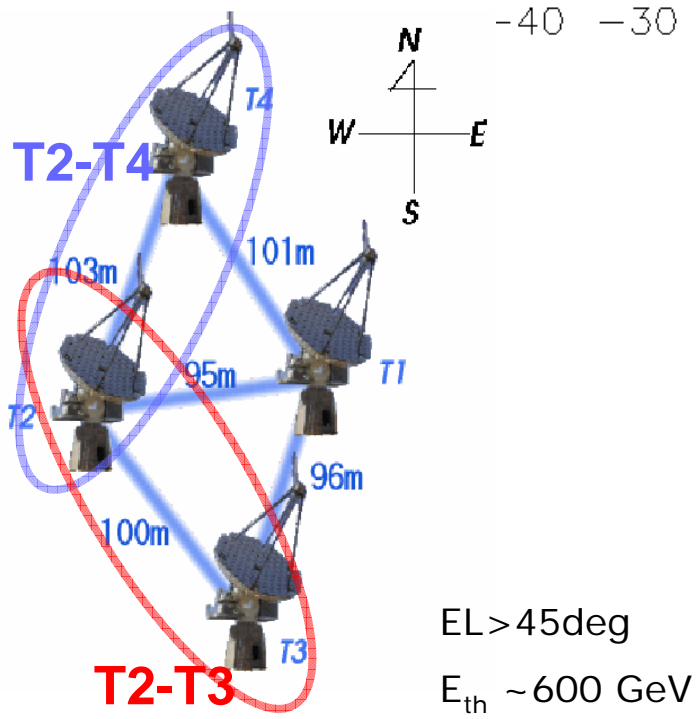
Observation term	Observation time (T2-T3)	Observation time (T2-T4)	Average zenith angle
15 – 28 Mar 2004	603 min	414 min	17 degree
15 – 28 Apr 2004	444 min	468 min	17 degree
Total	1047 min	882 min	

# Galactic diffuse emission



# Observation of the Galactic disk

M. Ohishi



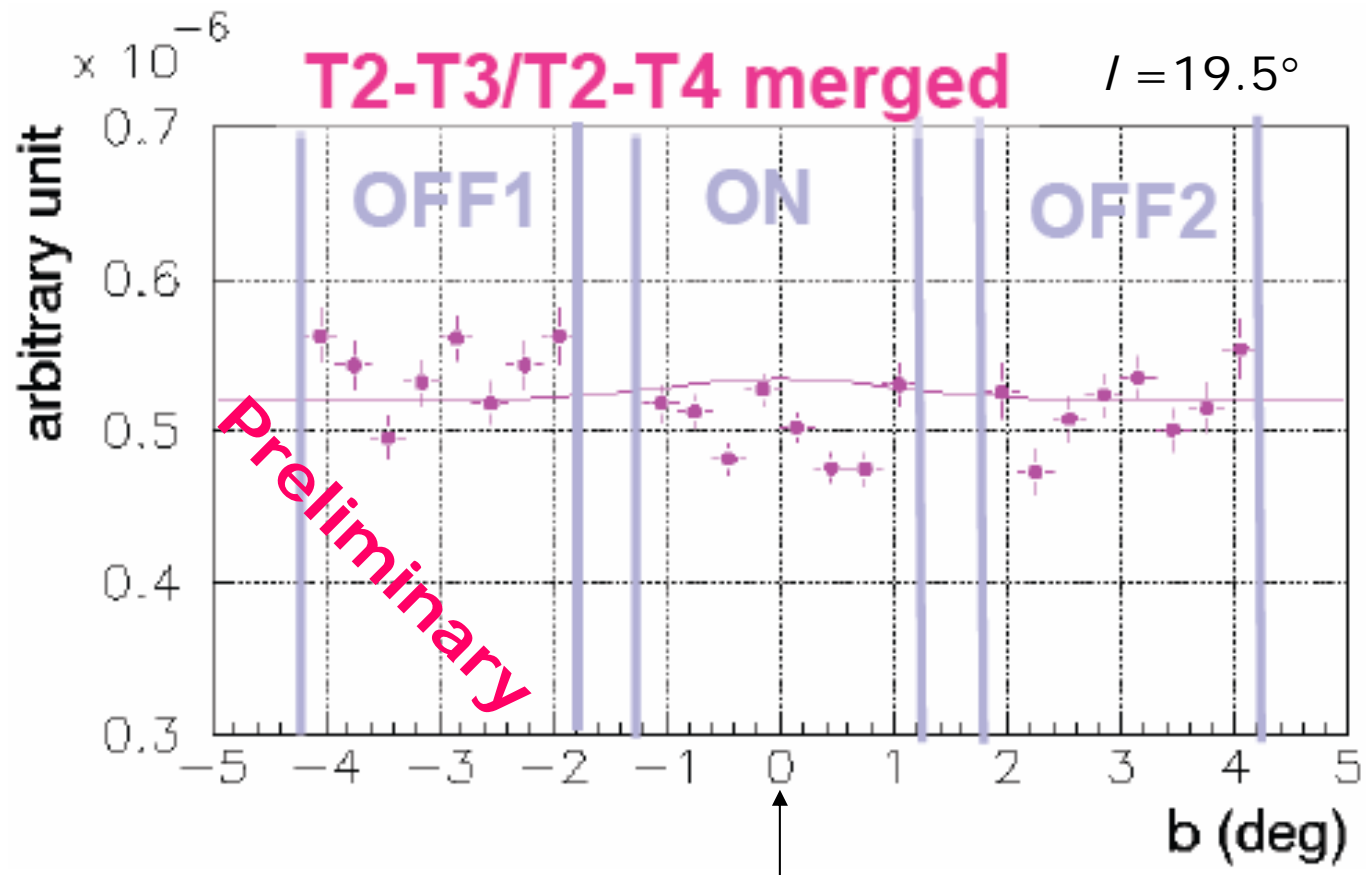
Obs. term	tel. pair	$b=0^\circ$	$b=-3^\circ$	$b=+3^\circ$
2004Jun	T2-T3	635.3	322.3	292.9
2004Jun	T2-T4	380.0	201.9	192.5

$I = +13$  2004Jun/Aug

Obs. term	tel. pair	ON	OFF
2004Jun	T2-T3	289.6	340.0
2004Jun	T2-T4	199.5	270.0
2004Aug	T2-T3	224.9	183.6
2004Aug	T2-T4	280.0	85.7

# Galactic disk scan result

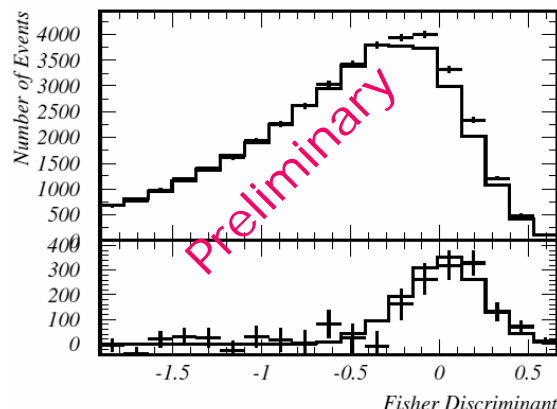
M. Ohishi



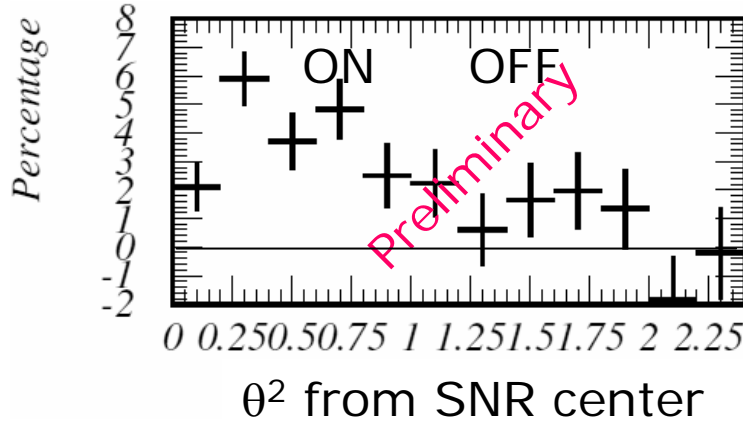
(expected  $\sigma \sim 1\text{deg}$ )

# SNR RX J0852.0-4622

In preparation

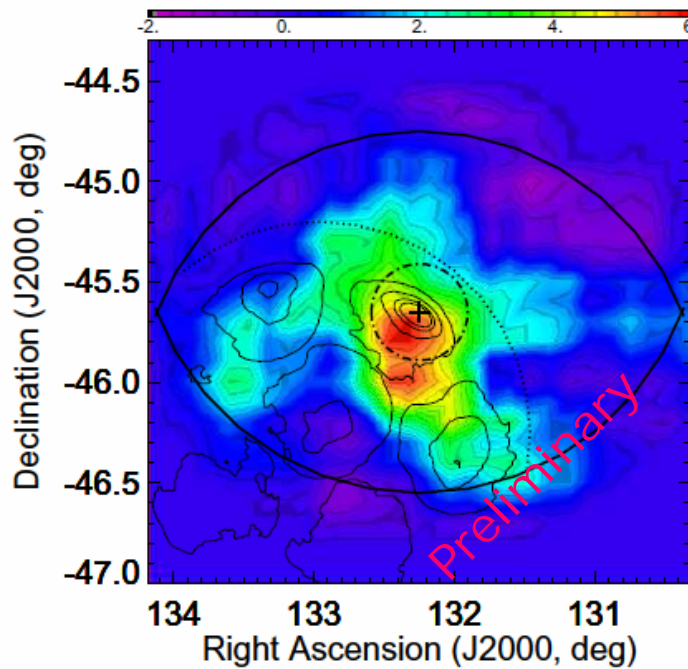


Fisher discriminant

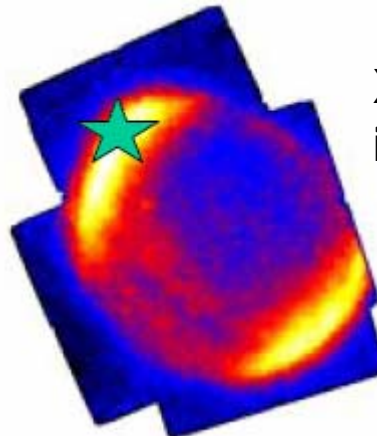


- T2 & T3 wobble
- 1,204 min. (2004 Jan/Feb)
- Off region: Vela or out of SNR

Excess event map

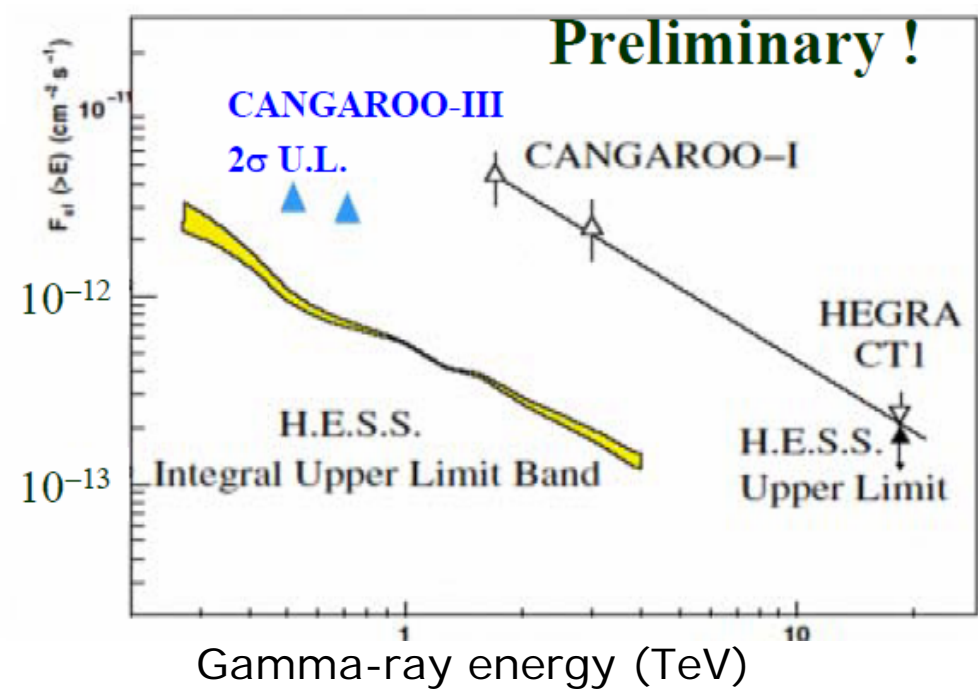
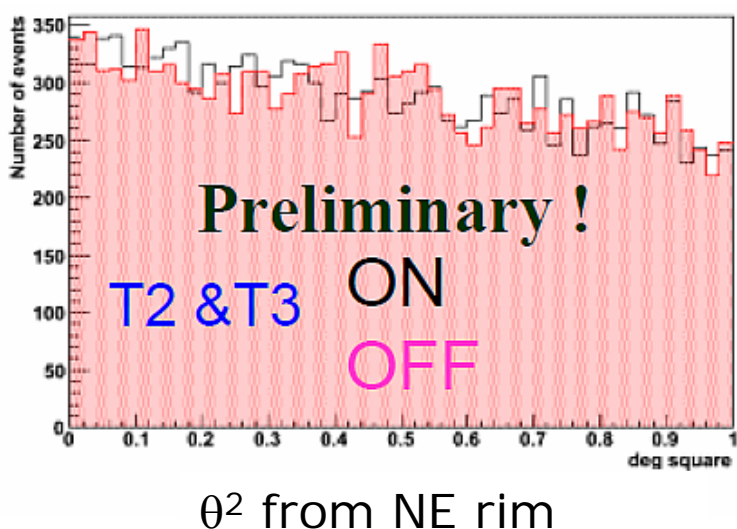


# SN1006 (G327.6+14.6)

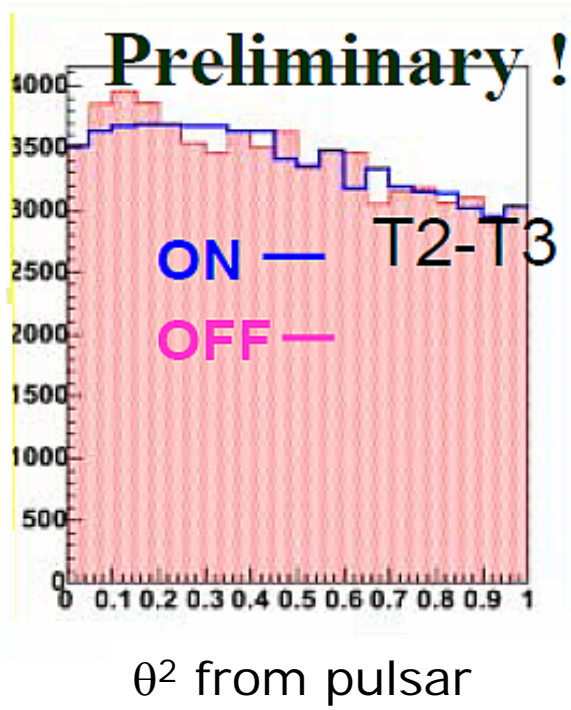
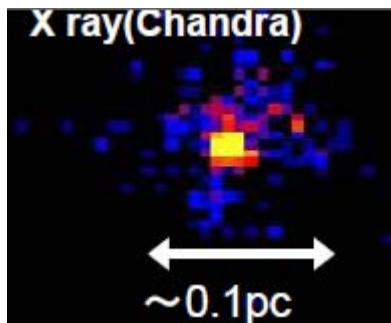


X-ray  
image  
(ASCA)

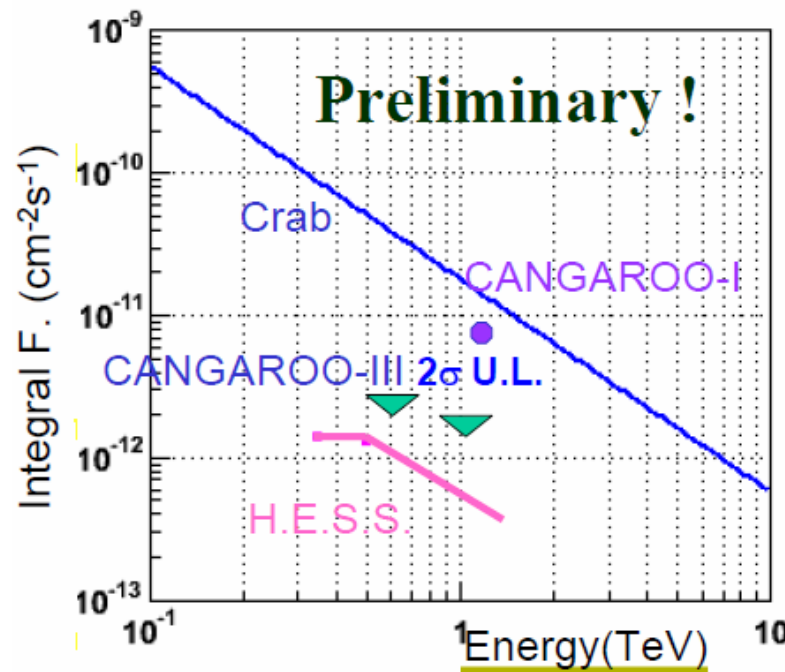
- NE-rim pointing (2004 May)
- T2, T3 & T4 long ON/OFF
- 1,625 min. ON, 1,738 min. OFF
- T2 & T3 results on likelihood
- Independent analysis (Fisher disc.)



# PSR 1706-44



- Pulsar pointing (2004 May)
- T2, T3 & T4 long ON/OFF
- 1,625 min. ON, 1,738 min. OFF
- T2 & T3 results on square cut
- Independent analysis (Fisher disc.)



## OG 2.7: New Experiments

### Cherenkov Telescopes

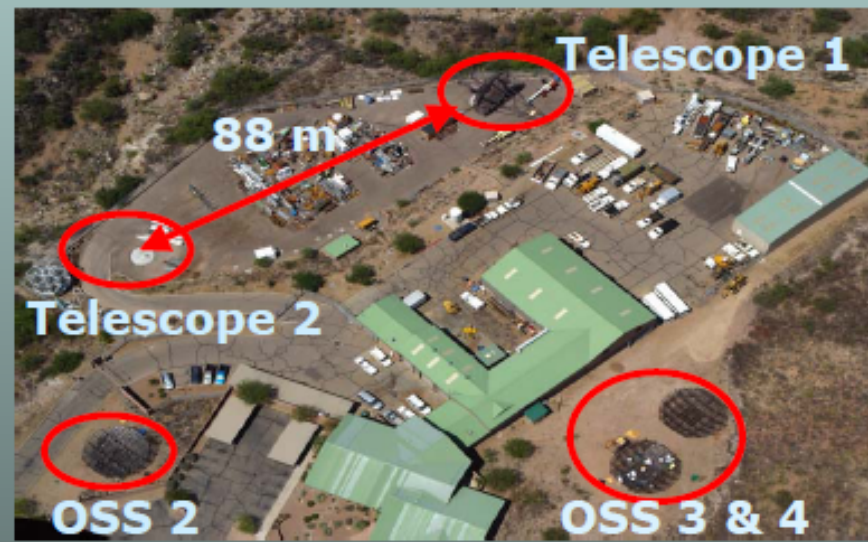
#### 1. VERITAS [Holder]

- 4x12m telescopes for Kitt Peak site → (2006).
- 2 telescopes operated this fall at Whipple Base Camp.



VERITAS  
Telescope 1

OG 1



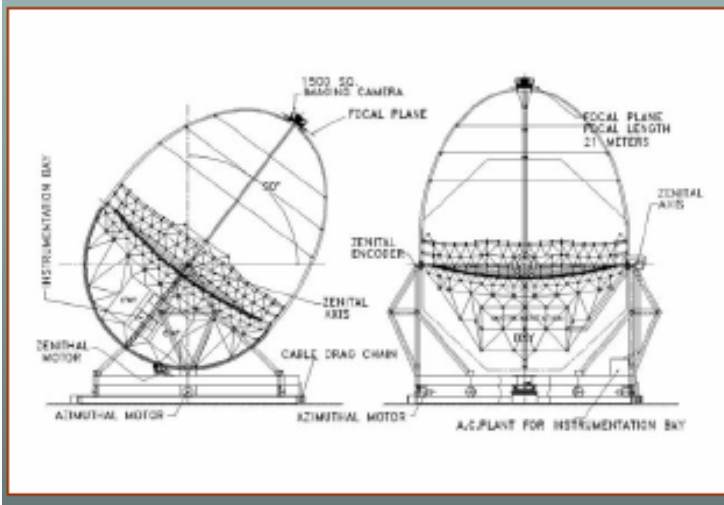
Page 61

## OG 2.7: New Experiments

### Cherenkov Telescopes

#### 2. HAGAR [Chitnis]

- 7 telescopes by late 2006.
- Hanle site, 4200m a.s.l.



#### 3. Mace [Koul]

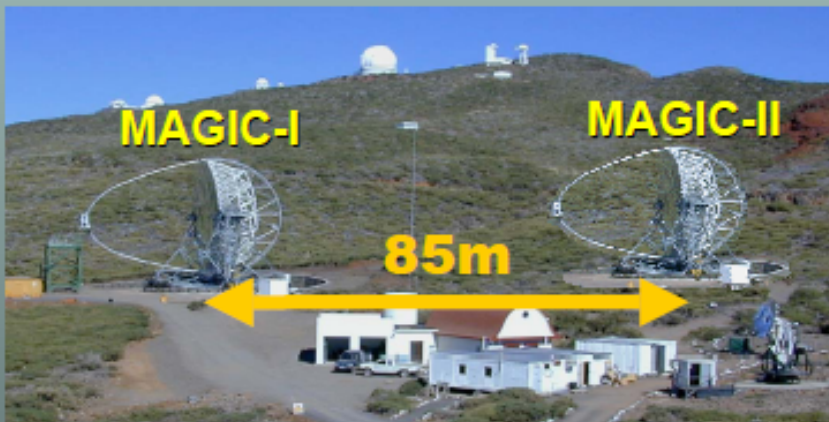
- 2 x 21m imaging telescopes.
- 4° x 4° camera.
- Hanle site.

## OG 2.7: New Experiments

### Cherenkov Telescopes

#### 4. HESS-II [Vincent]

- New 28m telescope.
- 2048 pixel camera.
- Lower energy 40-50 GeV.

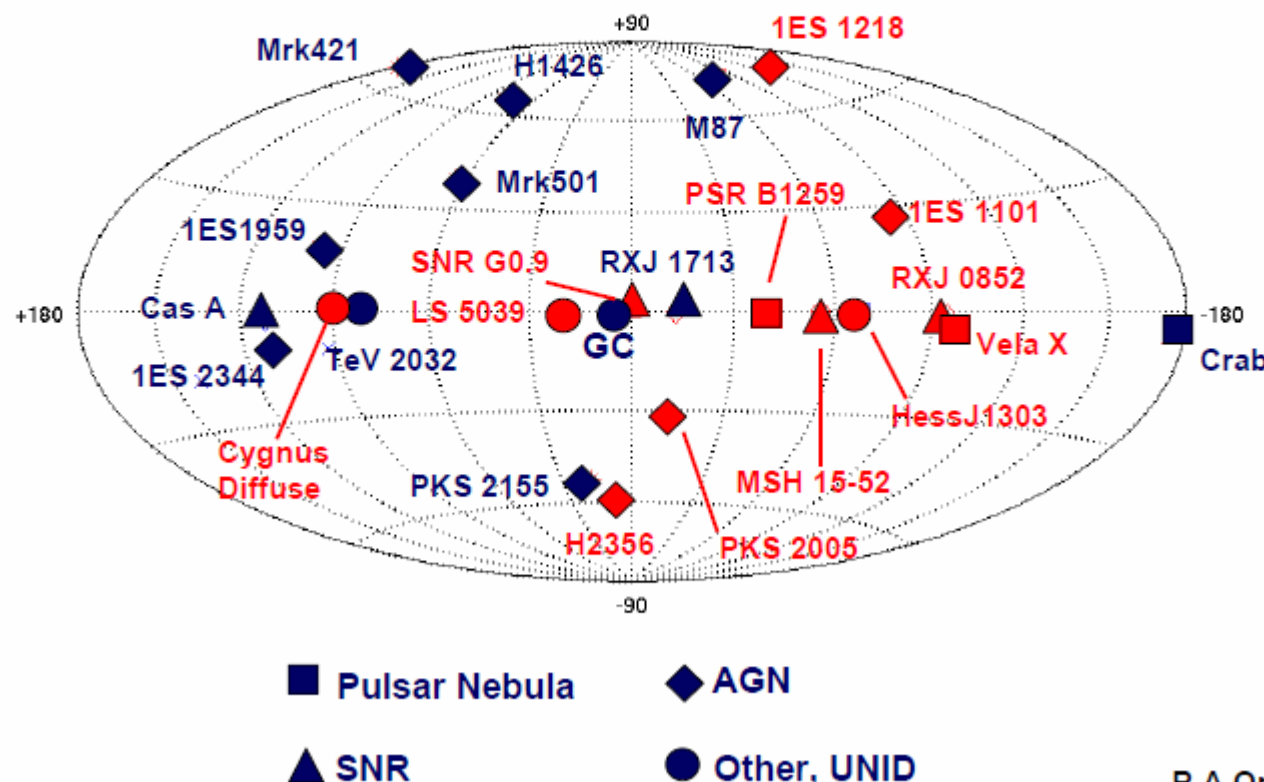


#### 5. MAGIC-II [Teshima]

- New 17m telescope.
- Possible high-QE camera.
- 2007 schedule.

# The VHE Sky - 2005

+ 8-15 add. sources  
in galactic plane.



R.A.Ong  
Aug 2005

# TeV Source Catalog

Name	RA	Decl	GL	GB	Claim	Comment	No.
NGC 253	11.888	-25.2882	97.369	-87.964	C2, ^H	Starburst Gal., z=0.00080	1
3C66A	35.66505	43.0855	140.143	-16.767	Cr	QSO, z=0.444	2
PSR0531+21	83.63288	22.01446	184.557	-5.785	Many	Crab pulsar/nebula	3
PSR0833-45	128.8359	-45.1766	263.552	-2.787	C1, ^H	Vela pulsar	4
RXJ0852.0-4622	132.2458	-45.6333	265.385	-1.181	C2, H	SNR, G266.6-1.2, Vela Jr.	5
Mkn 421	166.1138	38.20883	179.832	65.081	Many	XBL, z=0.081	6
Cen X-3	170.3132	-60.6233	292.09	0.336	D	X-ray binary	7
M87	187.7059	12.39112	283.778	74.491	H	Radio galaxy, z=0.00436	8
PSR1259-63/SS2883	195.6987	-63.8357	304.184	-0.992	H	PSR/Be binary	9
HESS J1303-631	195.7642	-63.1986	304.241	-0.356	H	UnID	10
H1426+428	217.1354	42.67361	77.49	64.899	Many	XBL, z=0.129	11
SN1006	225.5919	-41.8962	327.514	14.642	C1, ^H	SNR, G327.6+14.6	12
MSH15-52	228.5292	-59.1575	320.330	-1.192	C1, H	SNR, G320.4-1.2, HESS J1514-591	13
HESS J1614-518	243.5679	-51.8442	331.497	-0.594	H		14
HESS J1616-508	244.1083	-50.8964	332.394	-0.140	H	PSR J1617-5055?	15
HESS J1640-465	250.1829	-46.5319	338.317	-0.021	H	G338.3-0.0?	16
Mkn 501	253.4672	39.76004	63.6	38.859	Many	XBL, z=0.084	17
PSR1706-44	257.426	-44.4825	343.1	-2.683	C1, ^H	3EG J1710-4439	18
RXJ1713.7-3946	258.425	-39.7667	347.346	-0.498	C1, C2, H	SNR, G347.3-0.5	19
Sgr A*	266.4169	-29.0078	359.944	-0.046	C2, W, H	Gal.C. [Rogers et al.1994 ApJ434L59]	20
G0.9+0.1	266.8467	-28.1517	0.872	0.076	H	SNR	21
HESS J1804-216	271.1329	-21.6919	8.408	-0.027	H	G8.7-0.1 / W80?	22
HESS J1813-178	273.4079	-17.8428	12.813	-0.084	H	SNR AX J1813-178/AGPS273.4-17.8	23
HESS J1825-137	276.5150	-13.7633	17.820	-0.743	H	G18.0-0.7 ?	24
HESS J1826-148	276.5626	-14.8783	16.882	-1.289	H	LS 5089	25
HESS J1834-087	278.7104	-8.7533	23.258	-0.329	H	G23.3-0.3 / W41 ?	26
HESS J1837-069	279.4279	-6.9275	25.206	-0.121	H	G25.5+0.0 ?	27
1ES1959+650	299.9984	65.14852	98.003	17.67	U, W, HC	XBL, z=0.048	28
PKS2005-489	302.3721	-48.8219	350.386	-32.611	H	XBL, z=0.071	29
TeV J2082+4130	308.0292	41.50833	80.254	1.074	HC	UnID: Cyg OB2?	30
PKS2155-304	329.7169	-30.2256	17.73	-52.246	D, H	XBL, z=0.117	31
Cas A	350.8529	58.8154	111.736	-2.13	HC	SNR, G111.7-2.1	32
BL Lac	330.6807	42.27779	92.59	-10.441	Cr	z=0.0686	33
1ES2344+514	356.7702	51.70497	112.891	-9.908	W	XBL, z=0.044	34

Claim: W: Whipple, C1: CANGAROO-I, C2: CANGAROO-II, D: Durham, Cr: Crimea, HC: HEGRA CT, H: HESS., ^H: HESS. upper limit

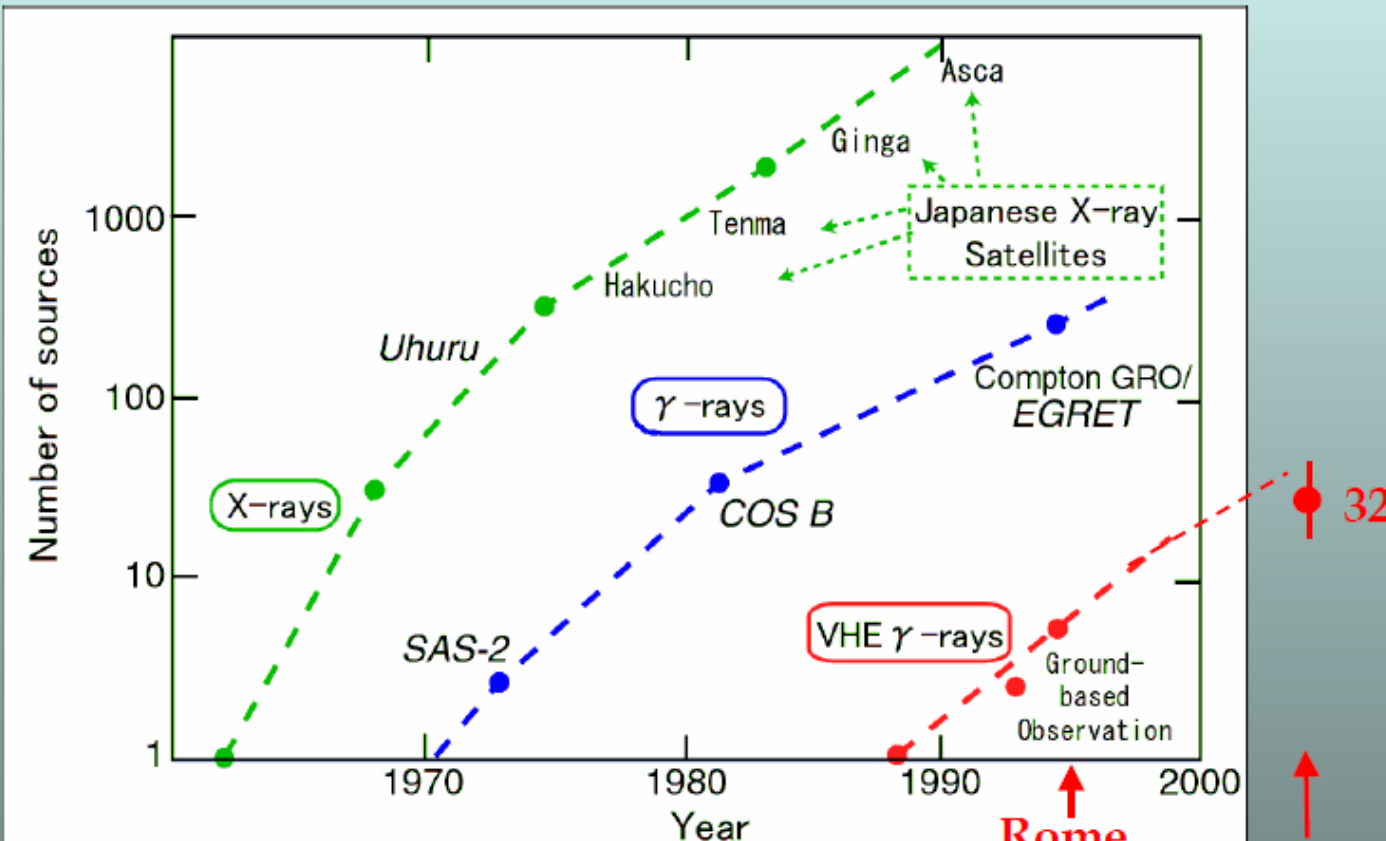
# Source Counts

Source Type*	2003	2005
Pulsar Wind Nebula (e.g. Crab, MSH 15-52 ...)	1	6
Supernova Remnants (e.g. Cas-A, RXJ 1713 ...)	2	6
Binary Pulsar (B1259-63)	0	1
Micro-quasar (LS 5039)	0	1
Diffuse (Cygnus region)	0	1
AGN (e.g. Mkn 421, PKS 2155 ...)	7	11
Unidentified	2	6
<b>TOTAL</b>	<b>12</b>	<b>32</b>

\* Includes likely associations of HESS unid sources.

→ Explosion in the number of VHE sources.

# “Kifune Plot”



Source count versus year  
[T. Kifune]

# Summary

---

- Detection of TeV gamma-rays from supernova remnants are confirmed, giving evidence for supernova origin of cosmic rays.
- CANGAROO-III 4-telescope stereo atmospheric Cherenkov telescopes are observing sub-TeV gamma-rays since 2004 March.
- Stereo analyses are being developed using local muons for calibration, and the energy spectrum of the Crab is consistent with other results.
- Observation of Vela pulsar showed no gamma-ray signal, but there is a hint of signal in the Vela X nebula.
- Preliminary results on Cen A and the Galactic disk show no gamma-ray signal. SNR RX J0852.0-4622 appears as extended source, and the morphological study is progressing.
- Observations of SN1006 and PSR1706-44 were made by using CANGAROO III telescopes. Preliminary analyses appear to show no significant signals, which may suggest upper limits lower than the CANGAROO-I fluxes obtained several years ago.
- The window of very-high-energy gamma-rays are opening up!